(NASA TN
TECHNICAL NOTE D-1987) OTS: $1.25

ANGULAR DISTRIBUTION OF EMITTED AND REFLECTED RADIANT ENERGY FROM DIFFUSE GRAY ASYMMETRIC GROOVES

By Morris Perlmutter and John R. Howell Washington, NASA, Oct. 1963
45 p refs

Lewis Research Center
Cleveland, Ohio

NATIONAL AERONAUTICS AND SPACE ADMINISTRATION

ANGULAR DISTRIBUTION OF EMITTED AND REFLECTED RADIANT ENERGY FROM DIFFUSE GRAY ASYMMETRIC GROOVES

By Morris Perlmutter and John R. Howell

SUMMARY

The directional emissivity and directional reflectivity of an infinitely long isothermal asymmetric groove with diffusely emitting and reflecting gray walls are analyzed, and numerical results are given. The directional emissivity is presented as a function of the groove parameters and material emissivity, while the directional reflectivity is presented as a function of these parameters and the angle of incident radiation. The directional reflectivity was found to be greatest at angles close to the angle of the incident beam, in sharp contrast to the commonly assumed diffuse or specular modes of reflection. The directional emissivity was greatest close to the angle bisecting the groove. The results thus indicate that the surface structure has a strong effect on the radiative properties. Some examples of radiant-energy interchange between surfaces with directional radiative properties are used to illustrate the large effects of these surfaces on the energy interchange. The examples also illustrate how the radiant interchange can be controlled to some extent by proper design of these surfaces. The analysis is restricted to grooves with dimensions that are large in comparison to the wavelengths of the radiation considered.

INTRODUCTION

The surface structure can have a strong influence on the reflective and emissive properties of materials. Not only can the absolute values of the emissivity and reflectivity be changed, but the emitted and reflected energy can be strongly directional because of the macroscopic surface structure. Calculation of radiant interchange between surfaces based on the usual assumptions of diffuse emissivity and specular or diffuse reflectivity can lead to large deviations from the actual values (refs. 1 to 3).

The particular surface configuration of asymmetric grooves was chosen to indicate this effect and to show how, by proper design of surfaces, the radiant heat transfer can be controlled to suit specific needs. Thus, it is possible by design of surface structure to exercise some control over radiant interchanges.

The model to be analyzed, shown in figure 1, consists of an infinitely long groove. One side of the groove is taken to be perpendicular to the base plane, the other to be at some angle θ from the vertical side. The wall surfaces are assumed to be gray and to emit and reflect diffusely. The environment is assumed

to have no effect except that there is incident radiation on the surface from an emitter at a given angle. In reference 1, the directional reflectivity and directional emissivity of a groove are treated when the walls of the groove are considered to be specularly, rather than diffusely, reflecting, as in the present case. The case of diffusely reflecting symmetric grooves is analyzed in references 4 to 6 for the total absorption and emission, but the directional emission and reflection are not considered.

In the present analysis, general equations for radiation from grooves are given. The general equations are separated into equations for directional emissivity and directional reflectivity. Both an exact and an approximate method of solution are given. In the approximate method, the groove surface is divided into large portions, each considered to have an average thermal flux.

SYMBOLS

A_1, A_2, A_3, A_4	defined in eqs. (A15) to (A18), respectively
dA_{B1}, dA_{B2}	area of flat black elements (fig. 2)
dA_C	area of cavity opening
D	offset distance of plate divided by distance between plates
$\Delta E, \Delta R$	width of emitter and receiver, respectively
e	energy ratio from groove wall, q_o/q_b
d^2F_{dA-dB}	shape factor from infinitesimal element at A to infinitesimal element at B
$\mathscr{F}$	exchange factor
H	height of groove wall normal to base plane
I_1, I_2	defined by eqs. (9) and (14)
K	kernel, $(\sin^2\theta)XY/(X^2 + Y^2 - 2XY \cos \theta)^{3/2}$
L	length of oblique groove wall
Q	thermal power; heat rate
q	thermal flux; heat rate per unit area
r	energy ratio reflected from groove wall, $q_o/[q_{oE}(\cos \eta')(\Delta\eta'/2)]$
T	absolute temperature of surface
X	distance along oblique side divided by H

Y distance along side normal to base plane divided by H

Z coordinate normal to XY-plane

α absorptivity

β angle between normal to X-surface and line from receiver to groove

β' angle between normal to X-surface and line from emitter to groove

ϵ emissivity

η angle between normal to base plane and line from groove to receiver, $\theta + \beta - (\pi/2)$, deg

η' angle between normal to base plane and line from groove to emitter, $\theta + \beta' - (\pi/2)$, deg

θ angle between walls of groove, deg

Ξ width of surfaces divided by distance between them; aspect ratio

ξ position along base plane

ρ reflectivity, $1 - \epsilon$

σ Stefan-Boltzmann constant

φ angle between normal to diagonal wall and line from point X to point Y

ω angle between normal to vertical side and line connecting points X and Y

Subscripts:

b black

C cavity

D diffuse surface

ΔE emitter

f flat surface

G groove

i total energy incident on a surface

l lower limit

o total energy out including both reflected and emitted energies

P perfect surface

ΔR receiver

r radiated

t total

u nonirradiated

w wall

X at point X

Y at point Y

ζ solution for reflectance

ξ solution for emittance

Superscripts:

$(\bar{})$ integrated average value

$(')$ incident beam

ANALYSIS

The model analyzed is shown in figure 1. There is a groove of infinite length in a plane. The short side of the groove is normal to the base plane and of height H and will be referred to as the Y-surface. The diagonal side is of length L and will be referred to as the X-surface. There is an open angle θ between the sides of the grooves. The surface of the groove walls is assumed gray with constant emissivity ϵ_w and constant wall temperature T_w. The reflection and emission from the wall are considered diffuse. The environment is assumed to have no effect.

Emitted and Reflected Energy from Groove

The rate of energy per unit area, thermal flux, leaving an element as X, can be expressed as

$$q_{oX} = q_w + \rho_w q_{iX} \tag{1}$$

where q_w is the energy emitted from the surface element at X, ρ_w is the reflectivity of the surface, and q_{iX} is the total incident flux. The flux is incident on the element at X from two sources, the Y-surface and an external source. The part of the thermal power per unit width leaving an infinite strip on Y, which is intercepted by the element dZ H dX at X, after using the re-

ciprocal relation $dX\ d^2F_{dX-dY} = dY\ d^2F_{dY-dX}$ is

$$q_{oY}\ dZ\ H\ dX\ d^2F_{dX-dY} \tag{2}$$

From reference 7, the shape factor is

$$d^2F_{dX-dY} = \frac{1}{2}\, d(\sin \varphi) \tag{3}$$

where φ is the angle between the normal to the X-surface and the line between the elements dX and dY. From figure 1 it can be found that

$$\sin \varphi = \frac{Y \cos \theta - X}{(Y^2 + X^2 - 2XY \cos \theta)^{1/2}} \tag{4}$$

and

$$d(\sin \varphi) = \frac{(\sin^2\theta)XY}{(Y^2 + X^2 - 2XY \cos \theta)^{3/2}}\, dY \equiv K(X,Y)dY \tag{5}$$

To get the total flux from Y incident on the element at X, equation (2) must be integrated between the limits $\sin \varphi|_{Y=0} = -1$ to $\sin \varphi|_{Y=1}$.

There is flux q_{oE} being radiated to the groove from an external source of width ΔE and of infinite length in the Z-direction. The angle between the normal to surface X and the beam from the emitter to X is β', as shown in figure 1. Assuming the distance between the emitter and the groove is large compared to the dimensions of the groove, the angle β' can be considered constant over all X. The power arriving at X from the emitter is

$$q_{oE}H\ dX\ dZ\ \frac{\cos \beta'}{2}\ \Delta\beta' \tag{6}$$

The total flux leaving an element at X is then

$$q_{oX} = q_w + \frac{\rho_w}{2} \int_0^1 q_{oY}K(X,Y)dY + \rho_w q_{oE} I_1(\beta', X)\Delta\beta' \tag{7}$$

where I_1 is equal to zero for the part of the X-surface that cannot see the emitter and $\cos \beta'/2$ for the part of the X-surface that can. An angle η' can be defined as the angle between the normal to the base plane and the incident beam. This can be shown to be

$$\eta' = \theta + \beta' - \frac{\pi}{2} \tag{8}$$

Thus, with each fixed η' from $-\pi/2$ to $+\pi/2$, I_1 will be zero on the X-

surface except in the cases

$$\left.\begin{array}{l}\theta > \eta' \geq 0;\ \text{all}\ \ X \\ 0 > \eta' > -\frac{\pi}{2};\ X > X_{l'}\end{array}\right\} I_1 = \frac{\cos\beta'}{2} \tag{9}$$

where $X_{l'}$ is the lower limit of the X-surface that can see the emitter and can be shown to be

$$X_{l'} = \frac{\cos(\theta + \beta')}{\cos\beta'} \tag{10}$$

It can be seen from equations (7) and (9) that q_{oX} is discontinuous at $X = X_{l'}$ in the cases where $0 > \eta' > -(\pi/2)$.

A procedure similar to that preceding can be carried out for the Y-wall to find q_{oY}. Let ω be the angle between the normal to Y and the line connecting X and Y as shown in figure 1. Then

$$\sin\omega = \frac{Y - X\cos\theta}{(X^2 + Y^2 - 2XY\cos\theta)^{1/2}} \tag{11}$$

$$d(\sin\omega) = -K(X,Y)dX \tag{12}$$

$$q_{oY} = q_w - \frac{\rho_w}{2}\int_{1/\cos\theta}^{0} q_{oX}K(X,Y)dX + \rho_w q_{oE}I_2(\beta',Y)\Delta\beta' \tag{13}$$

The term I_2 again depends on Y seeing the emitter; I_2 will be zero except in the following cases:

$$\left.\begin{array}{l}\theta \geq \eta' > 0;\ \text{all}\ \ Y \\ \frac{\pi}{2} \geq \eta' > \theta;\ Y > Y_{l'}\end{array}\right\} I_2 = -\frac{\cos(\theta + \beta')}{2} \tag{14}$$

where $Y_{l'}$ is the lower limit of surface Y that can see the emitter and is found by

$$Y_{l'} = \frac{\cos\beta'}{\cos\theta\cos(\beta' + \theta)} \tag{15}$$

As before, q_{oY} is discontinuous at $Y_{l'}$ for $\pi/2 > \eta' > \theta$.

Since equations (7) and (13) are linear, the problem can be separated into simpler parts that can be added for the complete solution. The term q_{oX} can be represented by the sum of two cases:

$$q_{oX} = q_{oX,\xi} + q_{oX,\zeta} \tag{16}$$

where $q_{oX,\xi}$ can be considered to be the total flux for the case in which there is no external source and the wall temperature of the groove is constant at T_w, and $q_{oX,\xi}$ is the total flux for zero wall temperature; that is, no emission from the wall, with an incident beam from an emitter at angle β'.

Similarly, q_{oY} is

$$q_{oY} = q_{oY,\xi} + q_{oY,\zeta} \tag{17}$$

Substituting equations (16) and (17) into equations (7) and (13) and letting the flux from the external source be zero give the solutions for emission from the groove. These may be nondimensionalized and expressed as e/ϵ, the total flux leaving the surface divided by the flux emitted from the surface:

$$\frac{e_X}{\epsilon_w} = \frac{q_{oX,\xi}}{q_w} = 1 + \frac{\rho_w}{2} \int_0^1 \frac{e_Y}{\epsilon_w} K(X,Y)dY \tag{18}$$

$$\frac{e_Y}{\epsilon_w} = \frac{q_{oY,\xi}}{q_w} = 1 + \frac{\rho_w}{2} \int_0^{1/\cos\theta} \frac{e_X}{\epsilon_w} K(X,Y)dX \tag{19}$$

If, instead, the wall temperature is held at zero, the solutions for reflection from the groove are

$$r_X = \frac{q_{oX,\zeta}}{q_{oE}(\cos\eta')\frac{\Delta\eta'}{2}} = \frac{2\rho_w I_1}{\cos\eta'} + \frac{\rho_w}{2} \int_0^1 r_Y K(X,Y)dY \tag{20}$$

$$r_Y = \frac{q_{oY,\zeta}}{q_{oE}(\cos\eta')\frac{\Delta\eta'}{2}} = \frac{2\rho_w I_2}{\cos\eta'} + \frac{\rho_w}{2} \int_0^{1/\cos\theta} r_X K(X,Y)dX \tag{21}$$

The term r is the ratio of flux reflected from the groove wall to total flux incident on the groove. Equations (18) to (21) can be combined by means of equations (16) and (17) to obtain the complete solution of emission and reflection from the groove wall.

Radiation to Receiver at a Given Direction from Groove

The power radiating from the surface of the groove in a particular direction to a receiver can be calculated as follows: A receiver of width ΔR and infinite in the Z-direction is located so that it will intercept the total radiation leaving the groove in a given direction β. The thermal power reaching the receiver from the part of an element of width dZ on side X directly visible to the receiver is

$$Q_{X-\Delta R} = H\, dZ\, \frac{\cos\beta}{2}\, \Delta\beta \int_{X_l}^{1/\cos\theta} q_{oX}\, dX \tag{22}$$

where β is the angle between the normal to side X and the line from X to the receiver. The receiver is considered to be far enough away in comparison to the dimensions of the groove so that β can be considered constant for all X. The lowest point on wall X that is visible to the receiver is X_l.

The power reaching the receiver from an element dZ on side Y is

$$Q_{Y-\Delta R} = -H\, dZ\, \frac{\cos(\theta+\beta)}{2}\, \Delta\beta \int_{Y_l}^{1} q_{oY}\, dY \tag{23}$$

The total power arriving at the receiver from one groove is then

$$Q_{G-\Delta R} = H\, dZ\, \frac{\cos\beta}{2}\, \Delta\beta \int_{X_l}^{1/\cos\theta} q_{oX}\, dX - H\, dZ\, \frac{\cos(\theta+\beta)}{2}\, \Delta\beta \int_{Y_l}^{1} q_{oY}\, dY \tag{24}$$

The limits on the integrals can be determined from the following:

$$\left.\begin{aligned} 0 < \eta < \theta: \quad & X_l = 0;\ Y_l = 0 \\ \theta \le \eta \le \tfrac{\pi}{2}: \quad & X_l = \frac{1}{\cos\theta};\ Y_l = \frac{\cos\beta}{\cos\theta\cos(\beta+\theta)} \\ -\tfrac{\pi}{2} \le \eta \le 0: \quad & X_l = \frac{\cos(\theta+\beta)}{\cos\beta};\ Y_l = 1 \end{aligned}\right\} \tag{25}$$

Again, $Q_{G-\Delta R}$ can be broken into two parts, one for emission and one for reflection:

$$Q_{G-\Delta R} = Q_{G-\Delta R,\xi} + Q_{G-\Delta R,\zeta} \tag{26}$$

The emission from a black surface on the base plane of area equal to the base of one groove that is incident on the receiver is

$$Q_{b-\Delta R} = q_b H\, dZ(\tan\theta)(\cos\eta)\, \frac{\Delta\eta}{2} \tag{27}$$

Using this to nondimensionalize $Q_{G-\Delta R,\xi}$ gives the directional emissivity

$$\epsilon_\eta = \frac{Q_{G-\Delta R,\xi}}{Q_{b-\Delta R}} = \frac{\cos\beta}{\cos\eta\tan\theta} \int_{X_l}^{1/\cos\theta} e_X\, dX - \frac{\cos(\theta+\beta)}{\cos\eta\tan\theta} \int_{Y_l}^{1} e_Y\, dY \tag{28}$$

which is the ratio of power reaching a receiver at angle η from the groove to that that would reach the receiver from a black groove. The power from the emitter incident on the base area $H\,dZ\tan\theta$ of one groove is

$$Q_{E-b} = q_{oE} H\,dZ(\tan\theta)(\cos\eta')\frac{\Delta\eta'}{2} \tag{29}$$

This is also the total power incident on a width dZ of the groove. Nondimensionalizing $Q_{G-\Delta R,\zeta}$ by equation (29) gives the directional reflectivity of the groove:

$$\rho_{\eta',\eta} = \frac{Q_{G-\Delta R,\zeta}}{Q_{E-b}} = \frac{\cos\beta}{\tan\theta}\frac{\Delta\eta}{2}\int_{X_l}^{1/\cos\theta} r_X\,dX - \frac{\cos(\theta+\beta)}{\tan\theta}\frac{\Delta\eta}{2}\int_{Y_l}^{1} r_Y\,dY \tag{30}$$

This directional reflectivity of the groove can be compared with the directional reflectivity $\left(\rho_{\eta',\eta}\right)_f$ of a flat diffuse surface with reflectivity ρ_w. This will be defined by

$$\left(\rho_{\eta',\eta}\right)_f = \rho_w(\cos\eta)\frac{\Delta\eta}{2} \tag{31}$$

Dividing equation (30) by equation (31) gives

$$\frac{\rho_{\eta',\eta}}{\left(\rho_{\eta',\eta}\right)_f} = \frac{\cos\beta}{\rho_w\cos\eta\tan\theta}\int_{X_l}^{1/\cos\theta} r_X\,dX - \frac{\cos(\theta+\beta)}{\rho_w\cos\eta\tan\theta}\int_{Y_l}^{1} r_Y\,dY \tag{32}$$

NUMERICAL SOLUTION

Equations (20) and (21) were solved for r_X and r_Y by an iterative numerical procedure. Initial values of r_Y were assumed and substituted into the integral in equation (20). This integral was then evaluated numerically to give values of r_X. These values were used in equation (21) to obtain new values of r_Y. This procedure was continued until convergence was obtained. A difficulty arose because of the integrand approaching infinity when both X and Y approached zero. This required the use of an analytical solution to evaluate r_X at X of zero and r_Y at Y of zero and the use of smaller increments of X and Y near zero. For some of the cases, there was a discontinuity in r_X or r_Y. This required that special care be taken in numerical integration through the discontinuity. The region was broken into two parts around the discontinuity, and each part was integrated separately. Increment sizes were reduced until

the solutions did not change.

After r_X and r_Y were obtained, they were substituted into equation (32), which was numerically integrated to give the directional-reflectivity ratio $\rho_{\eta',\eta}/(\rho_{\eta',\eta})_f$.

The method for finding e_X, e_Y, and ϵ_η follows a similar procedure. A discussion of an alternate approach for finding e_X and e_Y with a method for speeding convergence is given in reference 6.

Values of Emissivity and Reflectivity at X and Y of Zero

The limiting values of r and e can be found as follows: From equation (20), r_X at X of zero is

$$r_X\Big|_{X=0} = \frac{\rho_w}{2}\sin^2\theta \int_0^1 r_Y \frac{XY\,dY}{(X^2 + Y^2 - 2XY\cos\theta)^{3/2}}\Bigg|_{X=0} + \frac{2\rho_w I_1}{\cos\eta'} \tag{33}$$

The integral can be evaluated as in reference 4. There, it is clear that

$$r_X\Big|_{X=0} = \frac{\rho_w}{2} r_Y\Big|_{Y\to 0}(\cos\theta + 1) + \frac{2\rho_w I_2}{\cos\eta'} \tag{34}$$

$$r_Y\Big|_{Y=0} = \frac{\rho_w}{2} r_X\Big|_{X\to 0}(\cos\theta + 1) + \frac{2\rho_w I_2}{\cos\eta'} \tag{35}$$

and

$$e_X\Big|_{X=0} = \frac{\rho_w}{2} e_Y\Big|_{Y\to 0}(1 + \cos\theta) + \epsilon_w \tag{36}$$

$$e_Y\Big|_{Y=0} = \frac{\rho_w}{2} e_X\Big|_{X\to 0}(1 + \cos\theta) + \epsilon_w \tag{37}$$

The equations for $e_X\Big|_{X=0}$ and $e_Y\Big|_{Y=0}$ can then be simplified to give

$$e_X\Big|_{X=0} = e_Y\Big|_{Y=0} = \frac{\epsilon_w}{1 - \frac{\rho_w}{2}(1 + \cos\theta)} \tag{38}$$

Approximate Solutions for Emissivity

One means of obtaining an approximate solution is to assume constant average values of total emission over finite segments of the groove wall. For the simplest case, where the segment is equal to the length of the groove wall, the average value can be defined as follows:

$$\overline{e}_X \cong \cos\ \theta \int_0^{1/\cos\ \theta} e_X\ dX \tag{39}$$

$$\overline{e}_Y \cong \int_0^1 e_Y\ dY \tag{40}$$

As shown in appendix A, the approximate directional emissivity is then

$$\epsilon_\eta = \frac{(\cos\ \beta)\overline{e}_X}{(\tan\ \theta)\cos\ \eta}\left(\frac{1}{\cos\ \theta} - X_l\right) - \frac{\cos(\theta + \beta)\overline{e}_Y}{(\cos\ \eta)\tan\ \theta}(1 - Y_l) \tag{41}$$

where the values of X_l and Y_l are given by equations (10) and (15), respectively, after replacing β' by β. The values of $\overline{e}_X$ and $\overline{e}_Y$ are given by equations (A4) and (A5). A similar approximate method was used in reference 6 except that a linear variation over the segment was used rather than the wall emission being constant over the segment.

Approximate Solutions for Reflectivity

Approximate solutions for the reflectivity can be obtained in a somewhat similar manner. Since the part of the groove wall that is irradiated directly by the emitter will have a larger amount of energy reflected than the nonirradiated portion and since the reflected energy is also discontinuous at the junction between the irradiated and nonirradiated portions, it is necessary to divide the problem into separate mean values for the irradiated portion and for the remainder of each wall. These portions can again be subdivided for greater accuracy. For the simplest case of no subdivision of the segments, the mean values are

$$\left.\begin{aligned} \overline{r}_{Xr} &\cong \frac{1}{\left(\frac{1}{\cos\ \theta} - X_{l'}\right)} \int_{X_{l'}}^{1/\cos\ \theta} r_X\ dX \\ \overline{r}_{Xu} &\cong \frac{1}{X_{l'}} \int_0^{X_{l'}} r_X\ dX \end{aligned}\right\} \tag{42}$$

$$\left.\begin{aligned} \bar{r}_{Yr} &\cong \frac{1}{(1 - Y_{l'})} \int_{Y_{l'}}^{1} r_Y \, dY \\ \bar{r}_{Yu} &\cong \frac{1}{Y_{l'}} \int_{0}^{Y_{l'}} r_Y \, dY \end{aligned}\right\} \tag{43}$$

where $X_{l'}$ and $Y_{l'}$ are obtained from equations (10) and (15), respectively, and the subscripts r and u refer to the irradiated and nonirradiated segments, respectively. The ratio of the energy reflected to a receiver to that reflected by a flat diffuse surface is then, from equation (32) and appendix A,

$$\frac{\rho_{\eta',\eta}}{\left(\rho_{\eta',\eta}\right)_f} = \frac{\cos \beta}{\rho_w \cos \eta \tan \theta} \begin{bmatrix} \bar{r}_{Xr}\left(\frac{1}{\cos \theta} - X_{l'}\right) + \bar{r}_{Xu}(X_{l'} - X_l) & \text{if } X_{l'} > X_l \\ \bar{r}_{Xr}\left(\frac{1}{\cos \theta} - X_l\right) & \text{if } X_{l'} < X_l \end{bmatrix}$$

$$+ \frac{\cos(\theta + \beta)}{\rho_w \cos \eta \tan \theta} \begin{bmatrix} \bar{r}_{Yr}(1 - Y_{l'}) + \bar{r}_{Yu}(Y_{l'} - Y_l) & \text{if } Y_{l'} > Y_l \\ \bar{r}_{Yr}(1 - Y_{l'}) & \text{if } Y_{l'} < Y_l \end{bmatrix} \tag{44}$$

where the r terms are defined by equations (A7) to (A17).

The solution will depend on which part of the wall is illuminated, and so three regions are possible:

(1) When only part of wall X is illuminated $\left(0 > \eta' > -\frac{\pi}{2}\right)$, then $\bar{r}_{Yr} = 0$, $Y_{l'} = 1$, and $X_{l'} = \frac{\cos(\theta + \beta')}{\cos \beta'}$.

(2) When only part of wall Y is illuminated $\left(\frac{\pi}{2} > \eta' > \theta\right)$, then $\bar{r}_{Yr} = 0$, $X_{l'} = \frac{1}{\cos \theta}$, and $Y_{l'} = \frac{\cos \beta'}{\cos \theta \cos(\beta' + \theta)}$.

(3) When both X and Y are fully illuminated $(\theta > \eta' > 0)$, $\bar{r}_{Xu} = \bar{r}_{Yu} = 0$ and $X_{l'} = Y_{l'} = 0$.

Relations Between Directional Radiative Properties

The directional reflectivity can be related to both the directional emissivity and directional absorptivity by use of figure 2, as has been shown in reference 1 and is summarized in appendix B. This gives the relation

$$\epsilon_{C,\eta} = \alpha_{C,\eta} \tag{45}$$

The directional reflectivity may then be related to the directional emissivity as follows: The difference between the energy of the incident radiation from direction η' and the total reflected energy must be the energy absorbed by the groove. This can be written as

$$1 - \int_{-\pi/2}^{\pi/2} \frac{\rho_{\eta',\eta}}{\left(\rho_{\eta',\eta}\right)_f} \frac{\rho_w \cos \eta}{2} d\eta = \alpha_{\eta'} = \epsilon_{\eta'} \tag{46}$$

This equation was used to check the reflectivities and emissivities obtained in the numerical calculations. A reciprocal relation between the reflectivities is also obtained in appendix B. For the present geometry, the relation is

$$\frac{\rho_{\eta',\eta}}{\left(\rho_{\eta',\eta}\right)_f} = \frac{\rho_{\eta,\eta'}}{\left(\rho_{\eta,\eta'}\right)_f} \tag{47}$$

RESULTS

Emissivity Results

In figure 3 are shown e_X and e_Y, the total energy leaving a groove wall of emissivity ϵ_w compared with the emission from a black groove wall. In figure 3(a) this comparison is shown for groove angles θ of 15° and 60° with wall emissivity ϵ_w fixed at 0.1. It can be seen that e_X and e_Y become larger near X and Y of zero. This is due to multiple reflections increasing the apparent emission from the surface in this region. This effect is less apparent for the larger angle $\theta = 60^\circ$, and for this case the emission at the outer edge of the groove wall is close to the direct emission of the groove wall. In figure 3(b), the effect of varying emissivity ϵ_w is shown. This lower ϵ_w causes e_X and e_Y to rise sharply near X and Y of zero because of the increased interreflections at that point.

The directional emissivity ϵ_η is shown in figure 4 for various groove angles and wall emissivities. The directional emissivity is higher in every direction for the groove than for a flat wall of the same wall emissivity. The energy emitted in angles zero to θ is larger than that in other directions because of the interreflections at the base of the groove. The approximate solution yields curves that appear almost diffuse and deviate from the iterated solution. The approximate solution would be more correct if the groove wall were divided into segments.

Also shown is the directional emissivity from a symmetrical groove, calculated from results in reference 6. The values $e = e_X = e_Y$ were calculated from

values shown in reference 6.

The directional emissivity was then numerically calculated from

$$\epsilon_\eta = \frac{1}{2 \cos \eta \sin \frac{\theta}{2}} \left[\cos \beta \int_{X_\ell}^{1} e \, dX - \cos(\theta + \beta) \int_{Y_\ell}^{1} e \, dY \right] \tag{48}$$

which was derived similar to equation (28).

Reflectivity Results

In figure 5 is shown the thermal power reflected from the groove walls r_X and r_Y for both the approximate and the iterated solutions. The high value of r_Y for $\eta' = 60^\circ$ occurs where the wall is illuminated by the incident radiation. The discontinuity discussed earlier is evident.

The peak of r_X for a 60° incident beam occurs on the X-surface at an XH/L of about 0.63. This is the point on the X-surface that receives the greatest amount of power reflected from the directly illuminated portion of the Y-surface.

For the 1° incident beam, the entire groove surface is illuminated; however, the peaks of r_X and r_Y occur at X and Y of zero because of the many reflections at this point.

In figure 6, the directional-reflectivity ratio $\rho_{\eta',\eta} \Big/ \left(\rho_{\eta',\eta}\right)_f$ is presented for various incident beam angles η'. This is the ratio of the directional reflectivity of the groove to the directional reflectivity for a flat surface with the same diffuse reflectivity as the groove wall. The resulting reflectivity is neither specular nor diffuse. Instead, the energy is reflected most strongly in the direction of the incident beam.

The largest values of the directional-reflectivity ratio occur for the largest absolute value of incident angle, since, for those cases, the ratio of the illuminated area of the grooved surface to the area of the flat surface of comparison is a minimum.

The iterated directional reflectivities are plotted for comparison with the approximate solution, and the agreement for large absolute angles η' is seen to be good. In figure 7 is shown the effect of groove angle θ on the reflectivity ratio for various incident angles. When the groove angle is near 90°, the surface is practically flat, and the reflectivity ratio approaches 1.0.

The smaller values of the individual curves occur when only the unilluminated portion of the groove can be seen. The larger reflectivity ratio occurs when the receiver sees only the illuminated part of the groove.

In figure 7(a) the results for an incident beam at 1° are given. An almost diffuse reflectivity is obtained for θ of 89.9°.

In figure 8 is shown the effect of wall reflectivity on the groove directional-reflectivity ratio. The curves are similar in shape but show increasing values for increasing wall reflectivities.

BEHAVIOR OF SURFACES WITH DIRECTIONAL EMISSIVITY

To illustrate the use of directional surfaces in radiant interchange, the model shown in figure 9 is used. It consists of two semi-infinite parallel plates of dimensionless width Ξ separated by a distance 1. They are offset by a dimensionless distance D. The upper surface is black ($\epsilon_w = 1$) and at temperature T_b. The lower surface has a directional emissivity ϵ_η and is at temperature T_G. The surrounding environment is at temperature T_E. The net power transferred between the surfaces can be written following Hottel (ref. 8) as

$$Q_{bG} = \mathcal{F}_{bG} \Xi \, dZ\sigma\left(T_b^4 - T_G^4\right) \tag{49}$$

where $\mathcal{F}_{bG}$ is the net exchange factor. This exchange factor indicates the ability of two surfaces to exchange thermal power and is only dependent on their geometry and emissivity. In order to find $\mathcal{F}_{bG}$, it must be assumed for simplicity that the black surface is at $T_b = 0$; then the net power exchanged between the two surfaces is

$$Q_{Gb} = \sigma T_G^4 \, dZ \int_0^{\Xi} \int_{\eta_l}^{\eta_u} \left(\epsilon_\eta \frac{\cos \eta}{2} d\eta\right) d\xi \tag{50}$$

Using equation (49) and the reciprocal relation $A_1 \mathcal{F}_{1-2} = A_2 \mathcal{F}_{2-1}$ results in

$$\mathcal{F}_{bG} = \frac{1}{\Xi} \int_0^{\Xi} \int_{\eta_l}^{\eta_u} \left(\epsilon_\eta \frac{\cos \eta}{2} d\eta\right) d\xi \tag{51}$$

From figure 9, it can be seen that

$$\eta_l = \arctan(D - \xi) \tag{52}$$

$$\eta_u = \arctan(\Xi + D - \xi) \tag{53}$$

An additional relation can be obtained as follows: If the black surface and the environment are considered to be at $T = 0^\circ$ absolute, the emission from the directional surface will be the total of the emission to the black surface and the emission to the environment:

$$\mathcal{F}_{Gt} = \mathcal{F}_{Gb} + \mathcal{F}_{GE} = \frac{1}{\Xi\Xi} \int_0^{\Xi} \int_{-\pi/2}^{\pi/2} \left(\epsilon_\eta \frac{\cos \eta}{2} \, d\eta \right) d\xi \tag{54}$$

It can then be seen from equations (51) and (54) that

$$\mathcal{F}_{GE} = \frac{1}{\Xi\Xi} \int_0^{\Xi} \left[\int_{-\pi/2}^{\eta_l} + \int_{\eta_u}^{\pi/2} \left(\epsilon_\eta \frac{\cos \eta}{2} \, d\eta \right) \right] d\xi \tag{55}$$

For a good absorber, it is desirable to gain as much power from the black emitting surface and to lose as little energy to the environment as possible. This same condition would apply for a good emitter, where it is desirable for as much energy as possible to travel from the directional to the black surface, but as little as possible to travel to the environment.

Then, for a good absorbing or emitting directional surface, the following must be maximized:

$$\mathcal{F}_{bG} - \mathcal{F}_{GE} = \frac{1}{\Xi\Xi} \int_0^{\Xi} \left[\int_{\eta_l}^{\eta_u} - \int_{-\pi/2}^{\eta_l} - \int_{\eta_u}^{\pi/2} \left(\epsilon_\eta \frac{\cos \eta}{2} \, d\eta \right) \right] d\xi \tag{56}$$

This will be a maximum if a "perfect" absorber is assumed with $\epsilon_\eta = 1$ for $\eta_u > \eta > \eta_l$ and $\epsilon_\eta = 0$ otherwise. Then

$$\left(\mathcal{F}_{bG} - \mathcal{F}_{GE} \right)_P = \frac{1}{2\Xi} \left\{ \left[1 + (D + \Xi)^2 \right]^{1/2} + \left[1 + (D - \Xi)^2 \right]^{1/2} - 2(1 + D^2)^{1/2} \right\} \tag{57}$$

For a diffusely absorbing or emitting surface, $\epsilon_\eta = \epsilon_w$, a constant, to give

$$\left(\mathcal{F}_{bG} - \mathcal{F}_{GE} \right)_D = \epsilon_w \left[2 \left(\mathcal{F}_{bG} - \mathcal{F}_{GE} \right)_P \right] - 1 \tag{58}$$

In figure 10, the perfect and diffuse surfaces are compared with various directional surfaces.

It is also of interest to calculate the equilibrium temperature that these directional surfaces would attain if they were considered insulated from conduction and convection and were receiving radiation only from the black emitting surface. The environment is considered to be at $T_E = 0^\circ$ absolute. For this case,

$$\mathcal{F}_{Gb}\left(T_G^4 - T_b^4\right) + \mathcal{F}_{GE}T_G^4 = 0 \tag{59}$$

which becomes

$$\frac{T_G^4}{T_b^4} = \frac{\mathcal{F}_{bG}}{F_{G_t}} = \frac{1}{2 - \left(\frac{\mathcal{F}_{bG} - \mathcal{F}_{GE}}{F_{bG}}\right)} \tag{60}$$

The fraction T_G^4/T_b^4 is also the fraction of the total energy leaving the directional surface that reaches the black surface. For the diffuse case, equation (60) can be written as

$$\left(\frac{T_G}{T_b}\right)_D^4 = \frac{\left[1 + (\Xi + d)^2\right]^{1/2} + \left[1 + (\Xi - d)^2\right]^{1/2} - 2(1 + d^2)^{1/2}}{2\Xi} \tag{61}$$

and, for the perfect case, the temperature ratio $(T_G/T_b)^4$ is unity. The equilibrium temperature ratios for various cases are plotted in figure 11.

It is seen from figures 10 and 11 that it is possible to vary the heat exchange between surfaces by a large margin through proper design of the directional surface to attain the desired directional radiative properties.

In figure 10, for an offset distance of 1.0, it can be seen that surfaces with directional emissivities can be chosen as better absorbers or emitters than diffuse gray or black surfaces over certain ranges of Ξ. In figure 11, the equilibrium temperature ratio of the directional surfaces is always higher than that of a black diffuse surface for the case analyzed.

A surface with properties quite similar to those of a perfect surface is analyzed in reference 9.

CONCLUDING REMARKS

This analysis shows the large effects on radiative surface properties that surface irregularities may have. Since the wavelengths of thermal radiation may be quite small, the size of irregularities that can cause these effects is also small. Thus, great care must be taken in surface preparation of samples for measurement of radiative properties, as there can be significant differences between the apparent and actual properties.

The results show, too, that the directional radiative properties of surfaces can be controlled by design, and thus radiative interchange between bodies can also be controlled.

The usual assumption of diffuse emission is not true for grooved surfaces since the emissivity will be highest for directions bisecting the opening of the grooves. Similarly, the assumption of diffuse or specular reflections is not true since, in the case of grooves, the energy is primarily reflected in the direction of the incident beam.

Lewis Research Center
National Aeronautics and Space Administration
Cleveland, Ohio, June 24, 1963

APPENDIX A

APPROXIMATE SOLUTION

Approximate Solutions for Emissivity

One means of obtaining an approximate solution is to assume constant average values of total emission over finite segments of the groove wall. For the simplest case, where the segment is equal to the length of the groove wall, the average values can be defined by equations (39) and (40). Then, equations (18) and (19) become

$$\frac{\bar{e}_X}{\epsilon_w} = 1 + \frac{\rho_w \cos\theta}{2} \frac{\bar{e}_Y}{\epsilon_w} \int_0^{1/\cos\theta} \left(\int_{\sin\varphi|_{Y=0}}^{\sin\varphi|_{Y=1}} d \sin\varphi \right) dX \tag{A1}$$

$$\frac{\bar{e}_Y}{\epsilon_w} = 1 + \frac{\rho_w}{2} \frac{\bar{e}_X}{\epsilon_w} \int_0^{1} \left(\int_{\sin\omega|_{X=(1/\cos\theta)}}^{\sin\omega|_{X=0}} d \sin\omega \right) dY \tag{A2}$$

Evaluation of the integrals is simplified by noting that

$$\sin\varphi = \frac{df}{dX}$$
$$\sin\omega = -\frac{df}{dY} \tag{A3}$$

where $f = -(X^2 + Y^2 - 2XY\cos\theta)^{1/2}$. After evaluation at the limits, equations (A1) and (A2) become

$$\frac{\bar{e}_X}{\epsilon_w} = 1 + \frac{\rho_w}{2}\left(\frac{\bar{e}_Y}{\epsilon_w}\right)(\cos\theta - \sin\theta + 1) \tag{A4}$$

$$\frac{\bar{e}_Y}{\epsilon_w} = 1 + \frac{\rho_w}{2\cos\theta}\left(\frac{\bar{e}_X}{\epsilon_w}\right)(\cos\theta - \sin\theta + 1) \tag{A5}$$

Equations (A4) and (A5) are solved simultaneously. This same procedure would apply if each groove wall were divided into k increments, leading to a set of $2k$ equations in $2k$ unknowns, and would give more accurate results.

The emission picked up by a receiver can be found from equation (28) as

$$\epsilon_\eta = \frac{(\cos\beta)\bar{e}_X}{(\tan\theta)\cos\eta}\left(\frac{1}{\cos\theta} - X_l\right) - \frac{\cos(\theta+\beta)\bar{e}_Y}{(\cos\eta)\tan\theta}(1 - Y_l) \tag{A6}$$

where the values of X_l and Y_l are given by equations (10) and (15), respectively, after the replacement of β' with β.

Approximate Solutions for Reflectivity

Approximate solutions for the reflectivity can be obtained in a similar manner. Since the part of the groove wall that is irradiated directly by the emitter will have a larger amount of energy reflected than, and is discontinuous from, the nonirradiated portion, it is necessary to divide the problem into separate mean values for the irradiated portion and for the remainder of each wall. These portions can again be subdivided for greater accuracy. For the simplest case of no subdivision of the segments, the mean values are given by equations (42) and (43).

Equations (20) and (21) then become

$$\bar{r}_{Xr} = \frac{2\rho_w I_1}{\cos\eta'} + \left(\frac{1}{\cos\theta} - X_{l'}\right)^{-1}\int_{X_{l'}}^{1/\cos\theta}\frac{\rho_w}{2}\left(\bar{r}_{Yr}\int_{\sin\varphi|_{Y=Y_{l'}}}^{\sin\varphi|_{Y=1}} d\sin\varphi + \bar{r}_{Yu}\int_{\sin\varphi|_{Y=0}}^{\sin\varphi|_{Y=Y_{l'}}} d\sin\varphi\right)dX \tag{A7}$$

$$\bar{r}_{Xu} = \frac{1}{X_{l'}}\int_0^{X_{l'}}\frac{\rho_w}{2}\left(\bar{r}_{Yr}\int_{\sin\varphi|_{Y=Y_{l'}}}^{\sin\varphi|_{Y=1}} d\sin\varphi + \bar{r}_{Yu}\int_{\sin\varphi|_{Y=0}}^{\sin|_{Y=Y_{l'}}} d\sin\varphi\right)dX \tag{A8}$$

$$\bar{r}_{Yr} = \frac{2\rho_w I_2}{\cos\eta'} + \frac{1}{(1 - Y_{l'})}\int_{Y_{l'}}^{1}\frac{\rho_w}{2}\left(\bar{r}_{Xr}\int_{\sin\omega|_{X=(1/\cos\theta)}}^{\sin\omega|_{X=X_{l'}}} d\sin\omega + \bar{r}_{Xu}\int_{\sin\omega|_{X=X_{l'}}}^{\sin\omega|_{X=0}} d\sin\omega\right)dY \tag{A9}$$

$$\bar{r}_{Yu} = \frac{1}{Y_{l'}} \int_0^{Y_{l'}} \frac{\rho_w}{2} \left(\bar{r}_{Xr} \int_{\sin \omega|_{X=(1/\cos \theta)}}^{\sin \omega|_{X=X_{l'}}} d \sin \omega + \bar{r}_{Xu} \int_{\sin \omega|_{X=X_{l'}}}^{\sin \omega|_{X=0}} d \sin \omega \right) dY \tag{A10}$$

With the relations in equation (A3), the previous results can be integrated to

$$\bar{r}_{Xr} = \frac{\rho_w}{2} \left(\frac{1}{\cos \theta} - X_{l'} \right)^{-1} \left(\bar{r}_{Yr} A_1 + \bar{r}_{Yu} A_2 \right) + \frac{2\rho_w I_1}{\cos \eta'} \tag{A11}$$

$$\bar{r}_{Xu} = \frac{\rho_w}{2X_{l'}} \left(\bar{r}_{Yu} A_3 + \bar{r}_{Yu} A_4 \right) \tag{A12}$$

$$\bar{r}_{Yr} = \frac{\rho_w}{2(1 - Y_{l'})} \left(\bar{r}_{Xr} A_1 + \bar{r}_{Xu} A_3 \right) + \frac{2\rho_w I_2}{\cos \eta'} \tag{A13}$$

$$\bar{r}_{Yu} = \frac{\rho_w}{2Y_{l'}} \left(\bar{r}_{Xr} A_2 + \bar{r}_{Xu} A_4 \right) \tag{A14}$$

where

$$A_1 = \left(X_{l'}^2 + 1 - 2X_{l'} \cos \theta \right)^{1/2} + \left(Y_{l'}^2 + \frac{1}{\cos^2 \theta} - 2Y_{l'} \right)^{1/2} - \tan \theta - \left(X_{l'}^2 + Y_{l'}^2 - 2X_{l'} Y_{l'} \cos \theta \right)^{1/2} \tag{A15}$$

$$A_2 = \left(X_{l'}^2 + Y_{l'}^2 - 2X_{l'} Y_{l'} \cos \theta \right)^{1/2} - \left(Y_{l'}^2 - 2Y_{l'} + \frac{1}{\cos^2 \theta} \right)^{1/2} + \left(\frac{1}{\cos \theta} - X_{l'} \right) \tag{A16}$$

$$A_3 = \left(X_{l'}^2 + Y_{l'}^2 - 2X_{l'} Y_{l'} \cos \theta \right)^{1/2} - \left(X_{l'}^2 + 1 - 2X_{l'}^2 \cos \theta \right)^{1/2} + (1 - Y_{l'}) \tag{A17}$$

$$A_4 = (X_{l'} + Y_{l'}) - \left(X_{l'}^2 + Y_{l'}^2 - 2X_{l'} Y_{l'} \cos \theta \right)^{1/2} \tag{A18}$$

The terms $X_{l'}$, $Y_{l'}$, I_1, and I_2 are defined by equations (10), (15), (9), and (14), respectively.

The energy reflected to a receiver, then, from equation (32) is,

$$\frac{\rho_{\eta',\eta}}{\left(\rho_{\eta',\eta}\right)_f} = \frac{\cos\beta}{\rho_w \cos\eta \tan\theta}\left[\begin{array}{l}\bar{r}_{Xr}\left(\frac{1}{\cos\theta} - X_{l'}\right) + \bar{r}_{Xu}(X_{l'} - X_l) \quad \text{if} \quad X_{l'} > X_l \\ \\ \bar{r}_{Xr}\left(\frac{1}{\cos\theta} - X_l\right) \quad \text{if} \quad X_{l'} < X_l\end{array}\right]$$

$$+ \frac{\cos(\theta+\beta)}{\rho_w \cos\eta \tan\theta}\left[\begin{array}{l}\bar{r}_{Yr}(1 - Y_{l'}) + \bar{r}_{Yu}(Y_{l'} - Y_l) \quad \text{if} \quad Y_{l'} > Y_l \\ \\ \bar{r}_{Yr}(1 - Y_{l'}) \quad \text{if} \quad Y_{l'} < Y_l\end{array}\right] \qquad \text{(A19)}$$

APPENDIX B

RELATIONS BETWEEN GROOVE PROPERTIES

Consider a flat black element dA_{B1} and a cavity of arbitrary shape with an opening of area dA_C as shown in figure 2. These are in an isothermal enclosure. The radiative characteristics of the internal surface of the cavity are arbitrary. The radiation emitted from the black element and absorbed by the cavity is

$$Q_{B1-C} = \alpha_{C,\eta}\, dA_C\, d^2F_{C-B1} q_{B1} \tag{B1}$$

where the absorptivity $\alpha_{C,\eta}$ is the ratio of energy absorbed by the cavity to the energy incident on the cavity from dA_{B1}.

The energy radiated from the cavity to dA_{B1} and absorbed is

$$Q_{C-B1} = \epsilon_{C,\eta}\, d^2F_{C-B1} q_C\, dA_C \tag{B2}$$

Because both surfaces are at the same temperature, $q_C = q_{B1}$, and Q_{C-B1} must equal Q_{B1-C} since, from the second law of thermodynamics, there can be no net heat transfer between bodies at the same temperature. Thus,

$$\epsilon_{C,\eta} = \alpha_{C,\eta} \tag{B3}$$

A reciprocal relation between the reflectivities can also be obtained. Consider the isothermal cavity of figure 2 as containing two flat black elements dA_{B1} and dA_{B2} in addition to the cavity. The heat transferred from dA_{B1} to dA_{B2} by reflection from dA is

$$Q_{B1-B2} = q_{B1}\, d^2F_{C-B1}\, dA_C \rho_{C,\eta',\eta} \tag{B4}$$

Conversely, the radiation from dA_{B2} to dA_{B1} by reflection from dA is

$$Q_{B2-B1} = q_{B2}\, d^2F_{C-B2}\, dA_C \rho_{C\eta,\eta'} \tag{B5}$$

Because no net heat may be transferred between dA_{B1} and dA_{B2} when they are at the same temperature, and the direct interchange has been shown to be equal, it follows that $Q_{B1-B2} = Q_{B2-B1}$ and

$$\rho_{C,\eta',\eta}\, d^2F_{C-B1} = \rho_{C,\eta,\eta'}\, d^2F_{C-B2} \tag{B6}$$

For the geometry considered here and with the reflectivity ratios previously defined,

$$\frac{\rho_{\eta',\eta}}{\left(\rho_{\eta',\eta}\right)_f}\,\rho_w \cos\eta' \cos\eta \,\frac{d\eta'\,d\eta}{4} = \frac{\rho_{\eta,\eta'}}{\left(\rho_{\eta,\eta'}\right)_f}\,\rho_w \cos\eta \cos\eta' \,\frac{d\eta\,d\eta'}{4} \qquad \text{(B7)}$$

which reduces to

$$\frac{\rho_{\eta',\eta}}{\left(\rho_{\eta',\eta}\right)_f} = \frac{\rho_{\eta,\eta'}}{\left(\rho_{\eta,\eta'}\right)_f} \qquad \text{(B8)}$$

REFERENCES

1. Howell, John R., and Perlmutter, Morris: Directional Behavior of Emitted and Reflected Radiant Energy from a Specular, Gray, Asymmetric Groove. NASA TN D-1874, 1963.

2. Münch, Benjamin: Die Richtungsverteilung bei der Reflexion von Wärmestrahlung und ihr Einfluss auf die Wärmeübertragung. Mitteilung Nr. 16, Institut für Thermodynamik und Verbrennungs motorenbau an der Eidgenössischen Technischen Hochschule, Zurich, Mar. 16, 1955.

3. Polyak, G. G.: Radiative Transfer Between Surfaces of Arbitrary Spatial Distribution of Reflexions. Radiative Trans. Proj. Trans. TT-9, Purdue Univ., 1961.

4. Daws, L. F.: The Emissivity of a Groove. British Jour. Appl. Phys., vol. 5, no. 5, May 1954, pp. 182-187.

5. Sparrow, E. M., Gregg, J. L., Szel, J. V., and Manos, P.: Analysis, Results, and Interpretation for Radiation Between Some Simply-Arranged Gray Surfaces. Jour. Heat Transfer (Trans. ASME), ser. C, vol. 83, no. 2, May 1961, pp. 207-214.

6. Heaslet, Max A., and Lomax, Harvard: Numerical Predictions of Radiant Interchanges Between Conducting Fins with Mutual Irradiations. NASA TR R-116, 1961.

7. Jakob, Max: Heat Transfer. Vol. II. John Wiley & Sons, Inc., eq. 31-58, 1957.

8. Hottel, H. C.: Radiant-Heat Transmission. Heat Transmission, McAdams, W. H., ed., third ed., McGraw-Hill Book Co., Inc., 1954.

9. Perlmutter, Morris, and Howell, John R.: A Strongly Directional Emitting and Absorbing Surface. Jour. Heat Transfer (Trans. ASME), ser. C, vol. 85, no. 3, Aug. 1963, pp. 282-283.

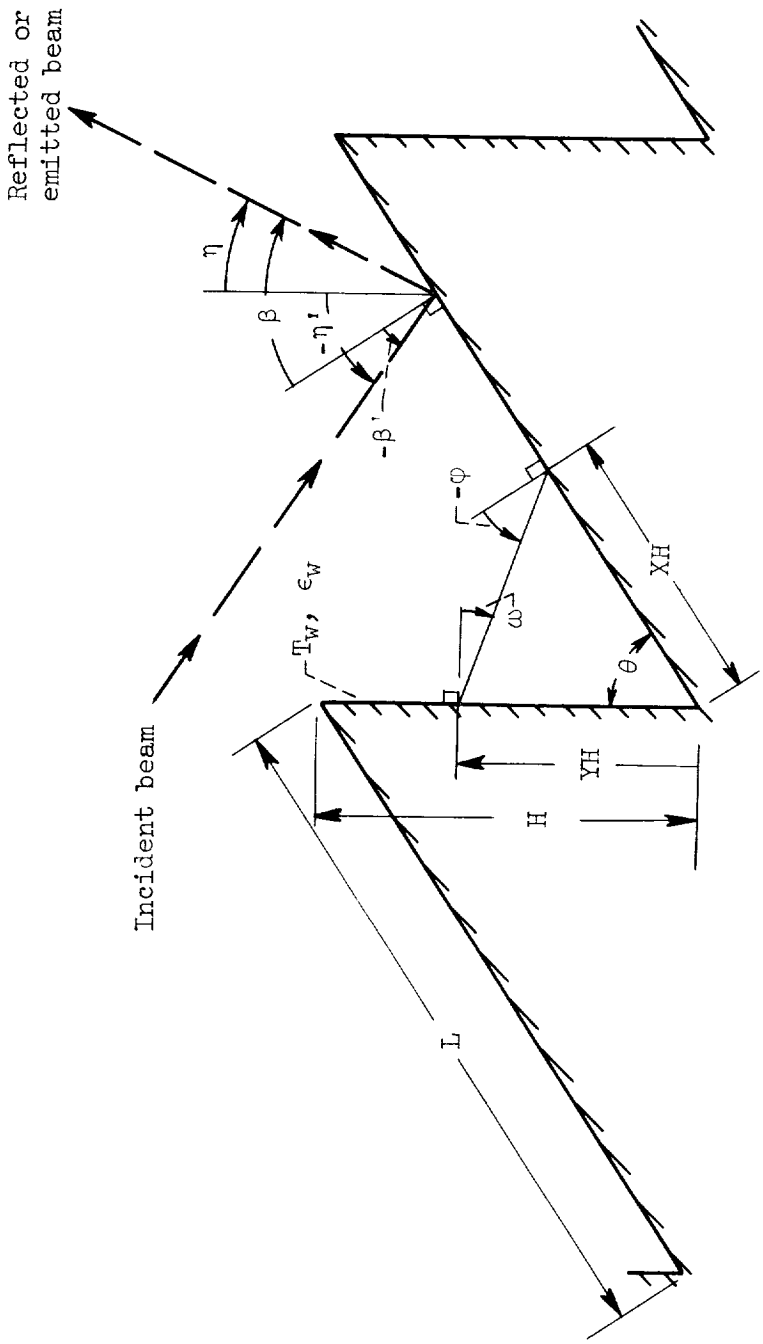

Figure 1. - Groove geometry.

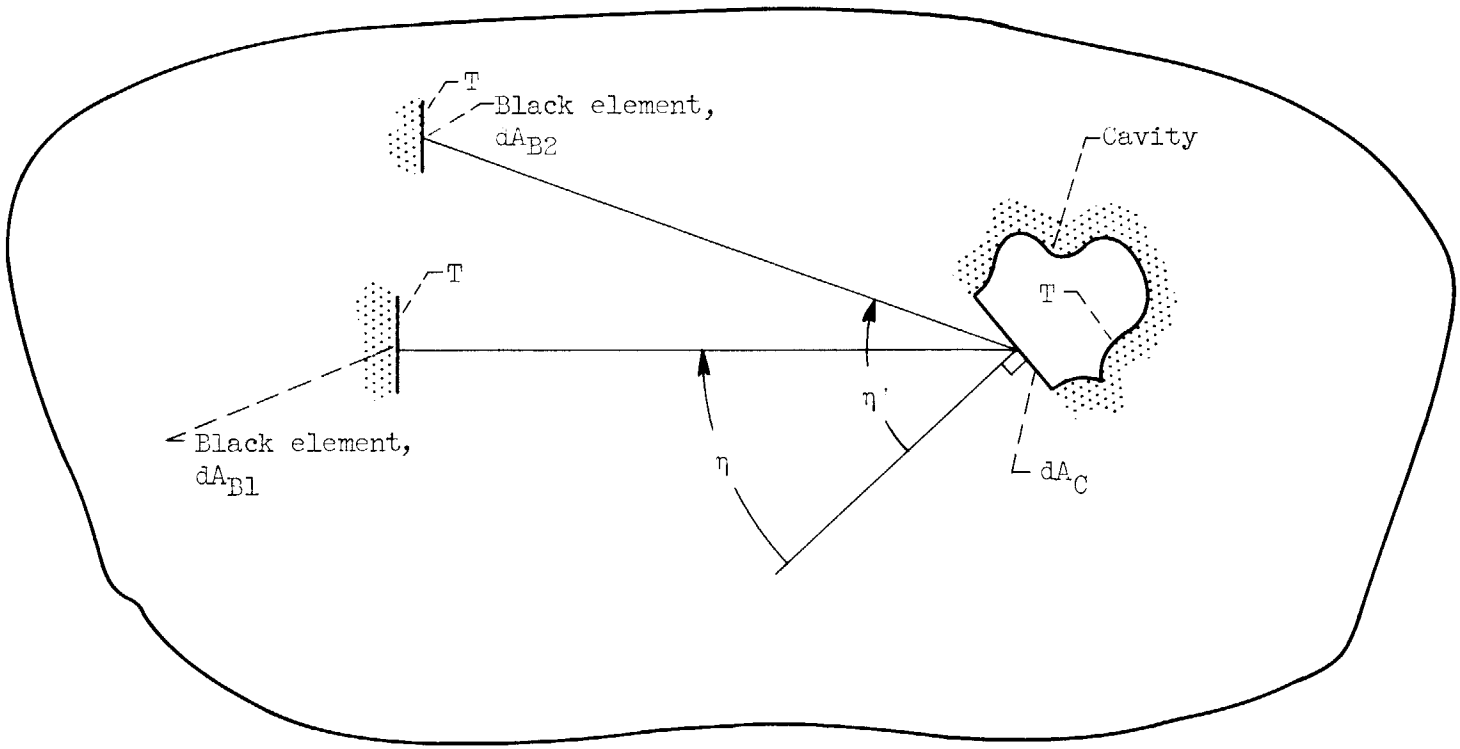

Figure 2. - Isothermal enclosure with flat black elements and isothermal cavity all at temperature T.

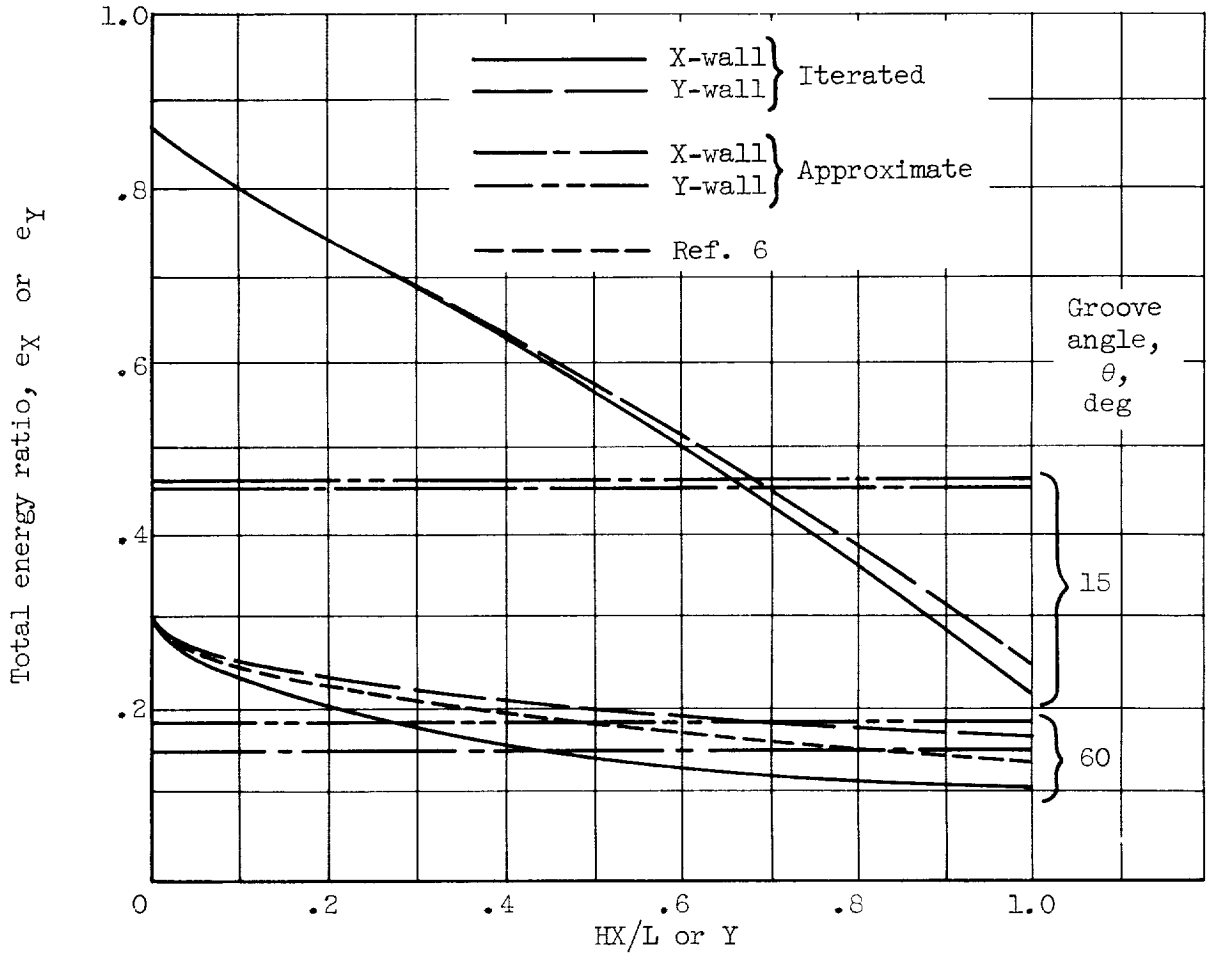

(a) Wall emissivity, 0.1

Figure 3. - Total energy ratio leaving groove wall for emittance case.

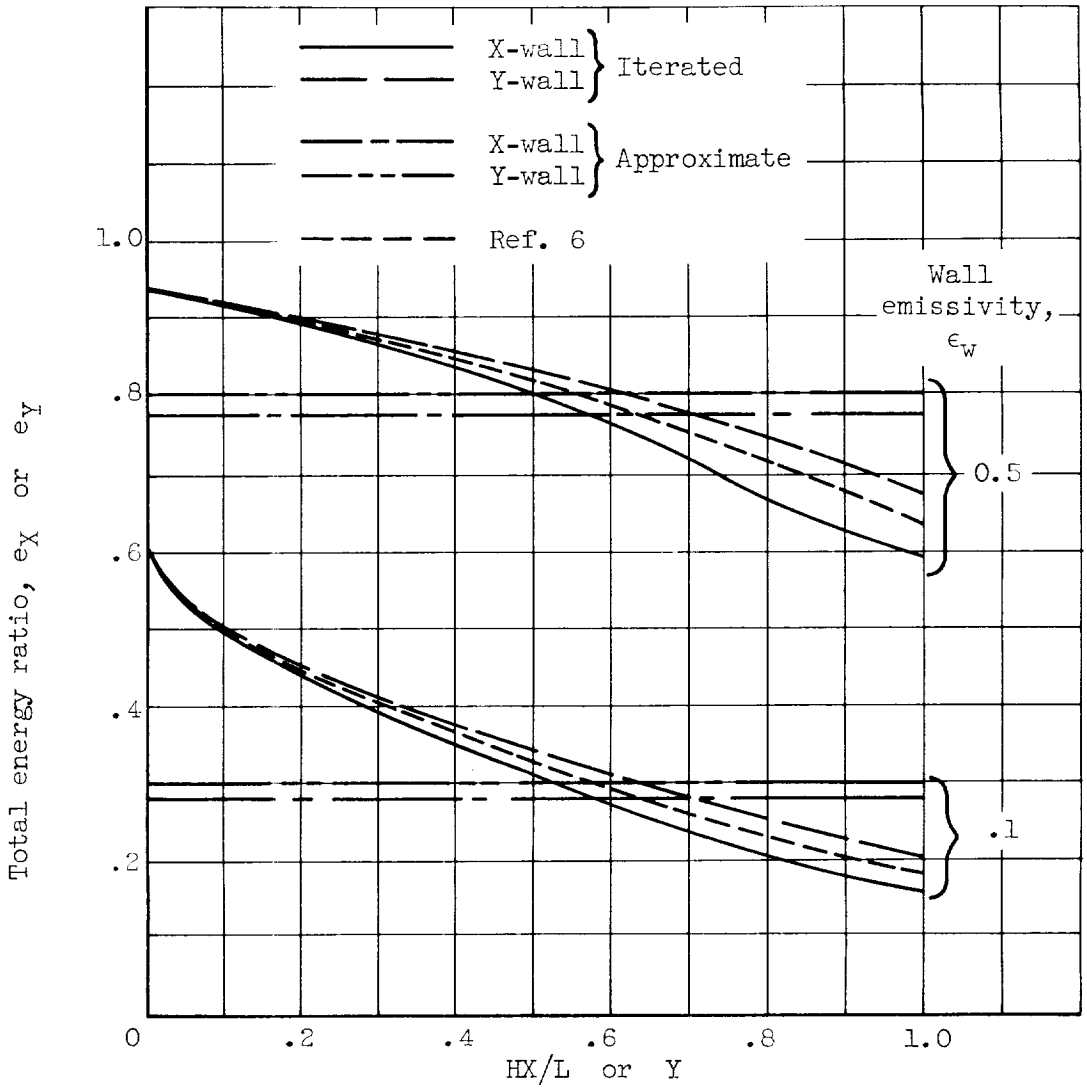

(b) Groove angle, 30°.

Figure 3. - Concluded. Total energy ratio leaving groove wall for emittance case.

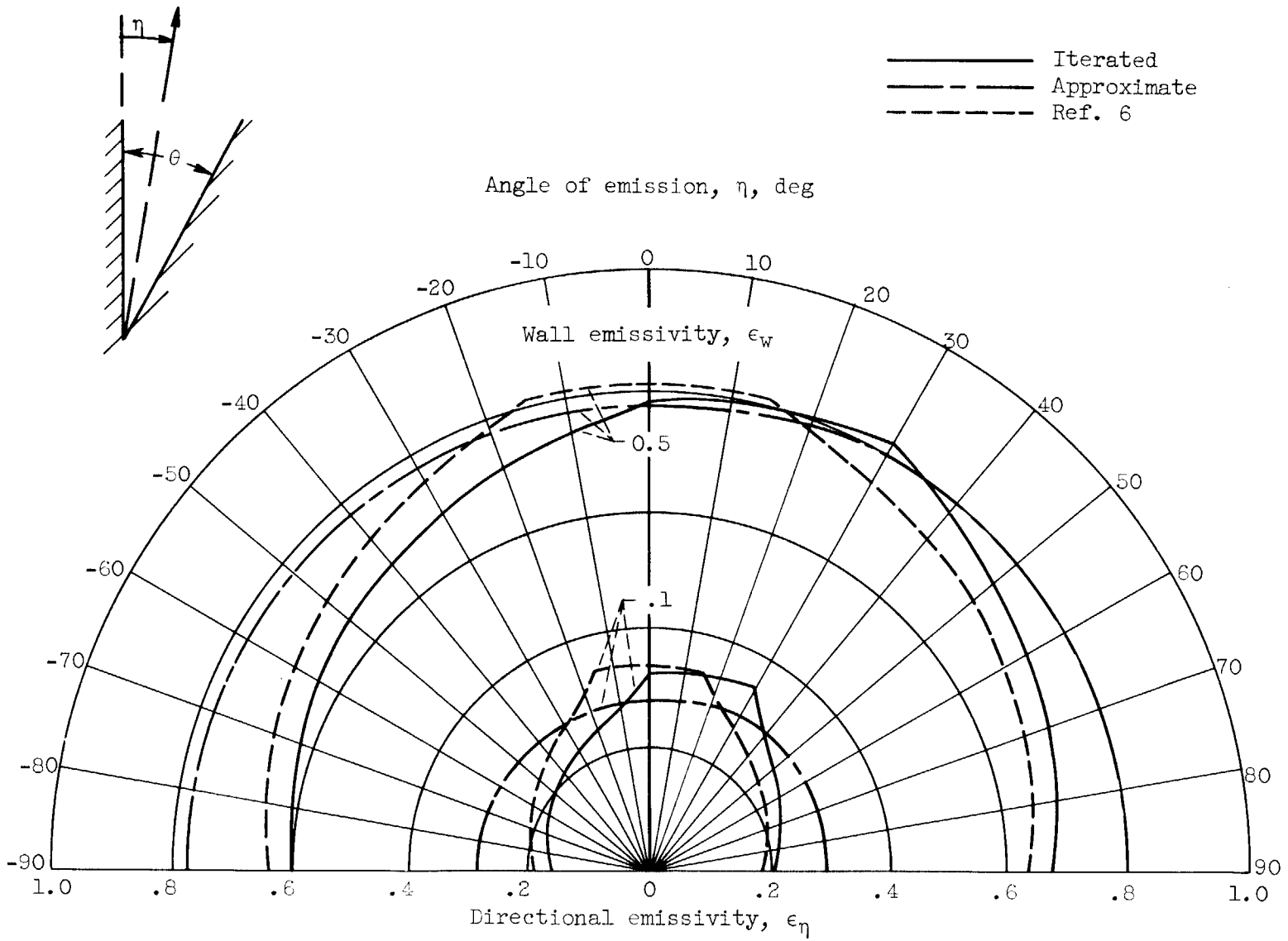

(a) Groove angle, 30°.

Figure 4. - Directional emissivity from groove.

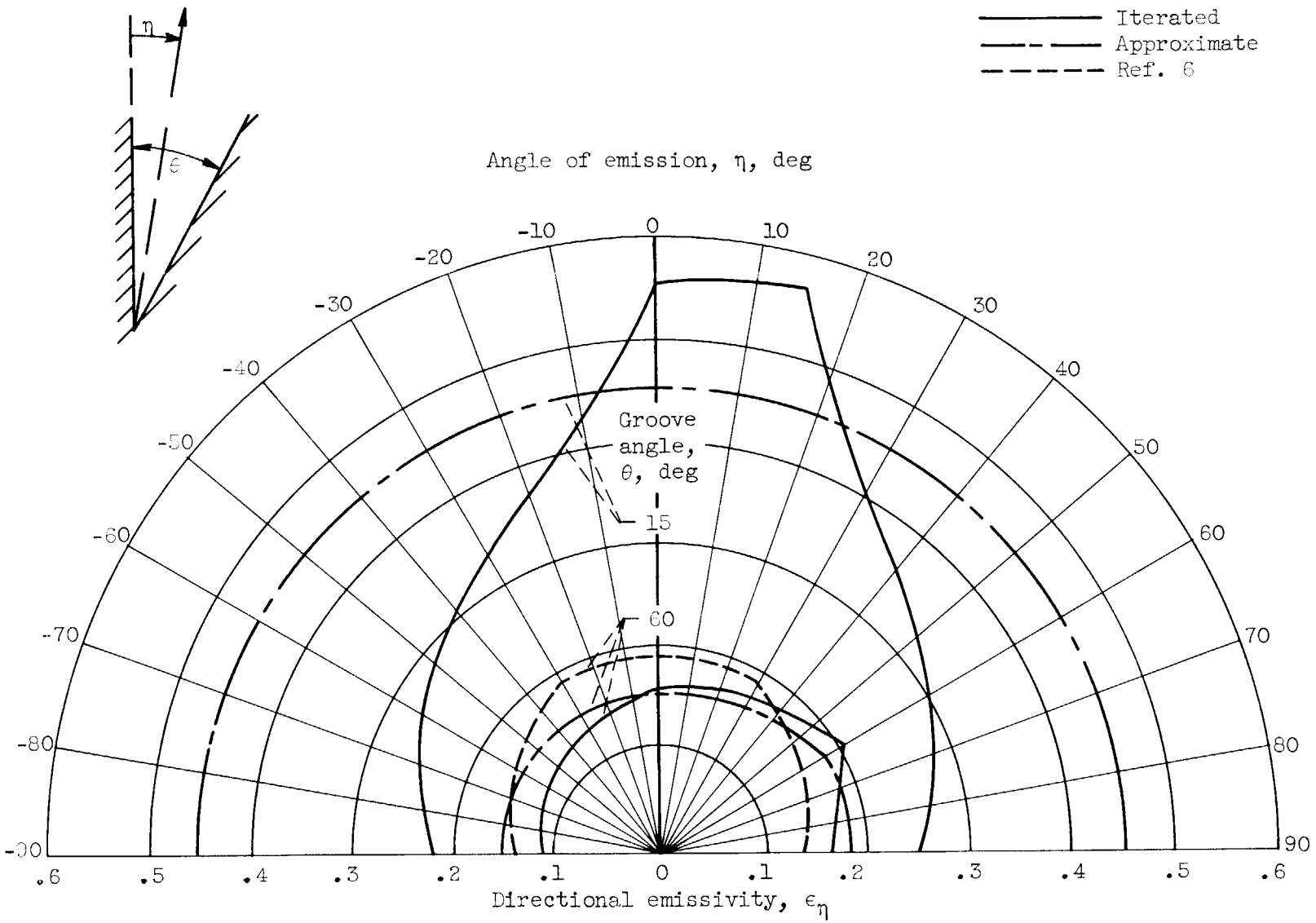

(b) Wall emissivity, 0.1.

Figure 4. - Concluded. Directional emissivity from groove.

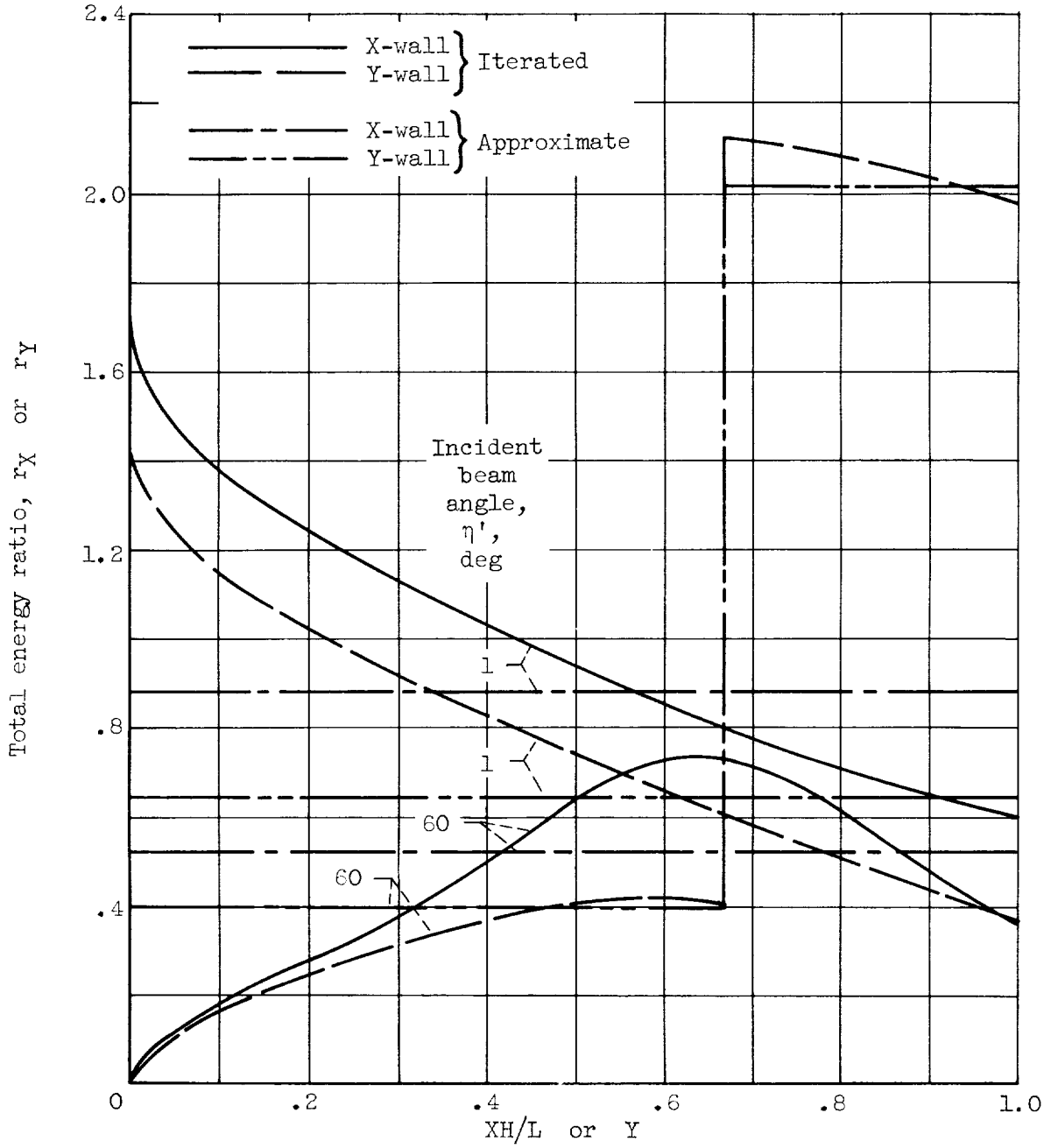

Figure 5. - Total energy ratio leaving groove wall for reflective case. Groove angle, 30°; wall reflectivity, 0.9.

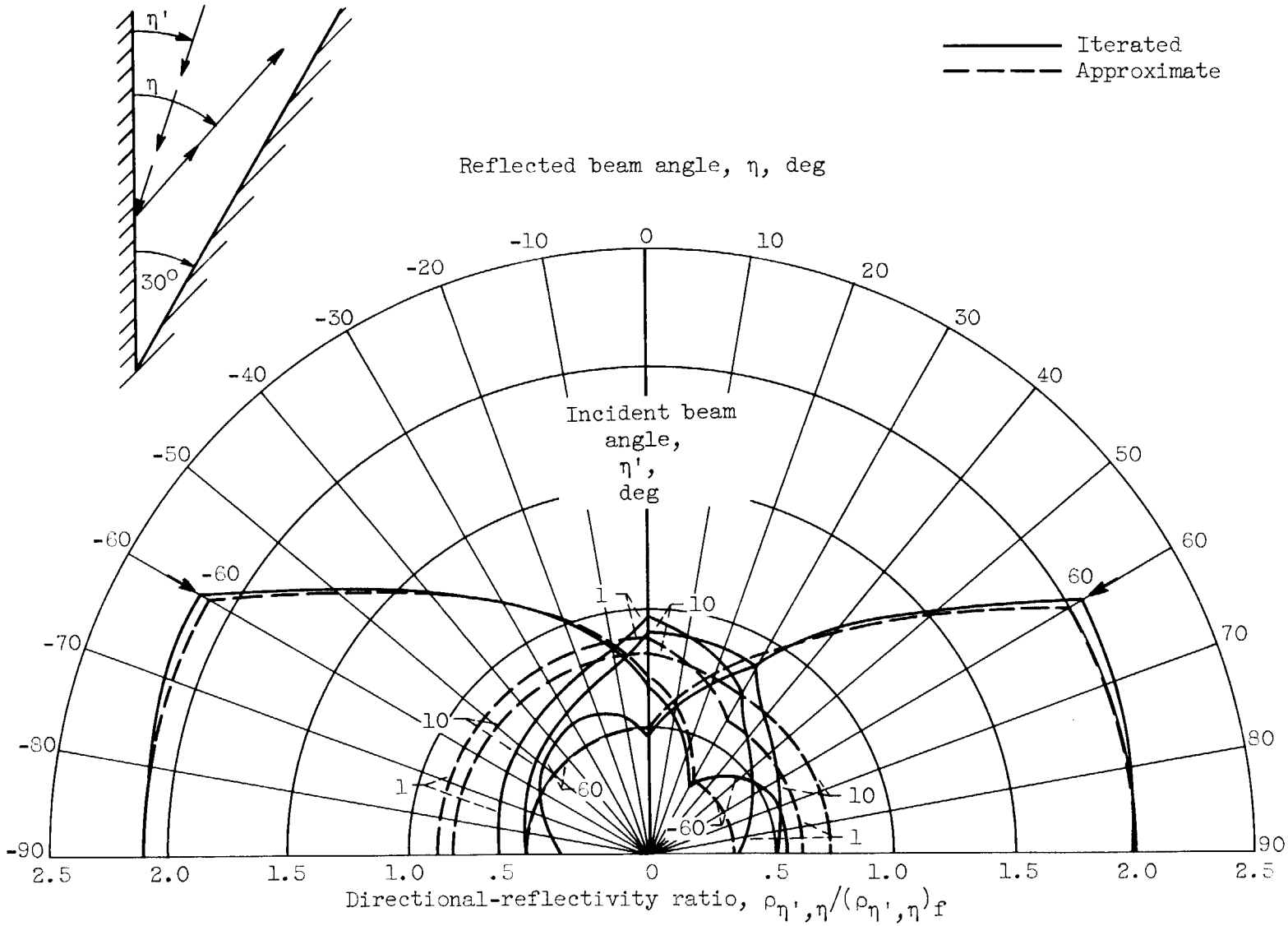

Figure 6. - Effect of incident beam angle on directional-reflectivity ratio. Wall reflectivity, 0.9; groove angle, 30°.

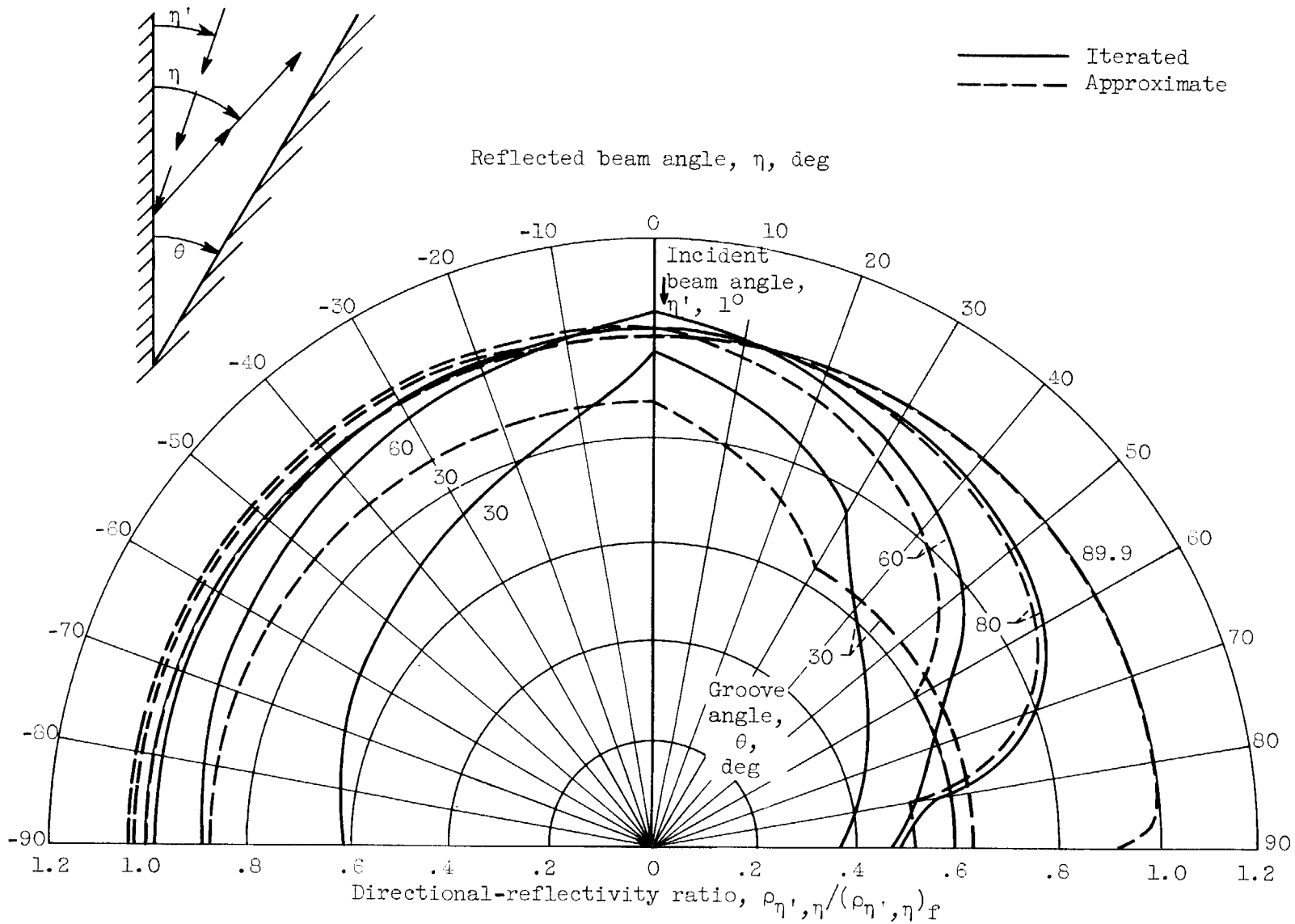

(a) Incident beam angle, 1°.

Figure 7. - Effect of groove angle on directional-reflectivity ratio. Wall reflectivity, 0.9.

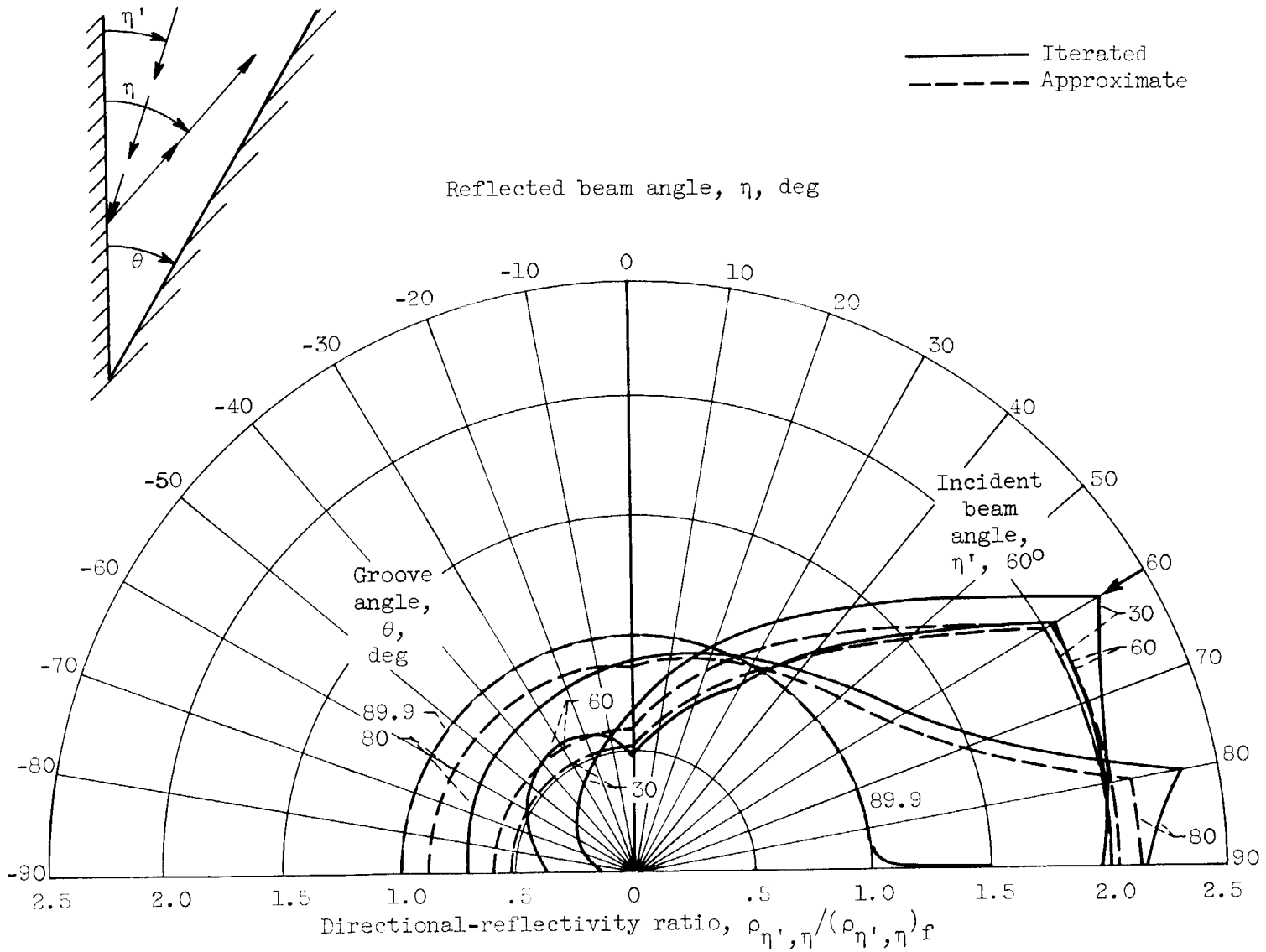

(b) Incident beam angle, 60°.

Figure 7. - Continued. Effect of groove angle on directional-reflectivity ratio. Wall reflectivity, 0.9.

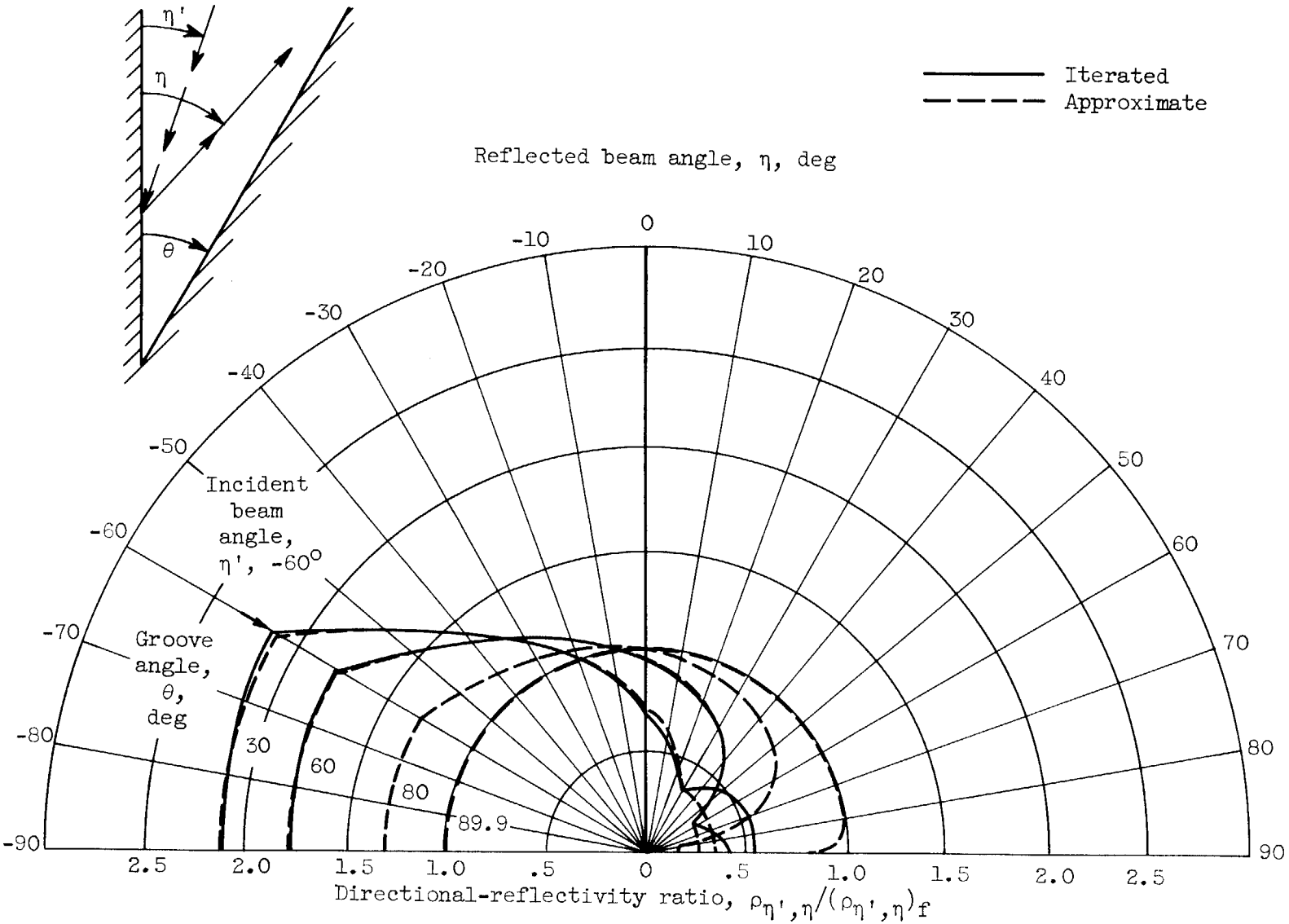

(c) Incident beam angle, -60°.

Figure 7. - Concluded. Effect of groove angle on directional-reflectivity ratio. Wall reflectivity, 0.9.

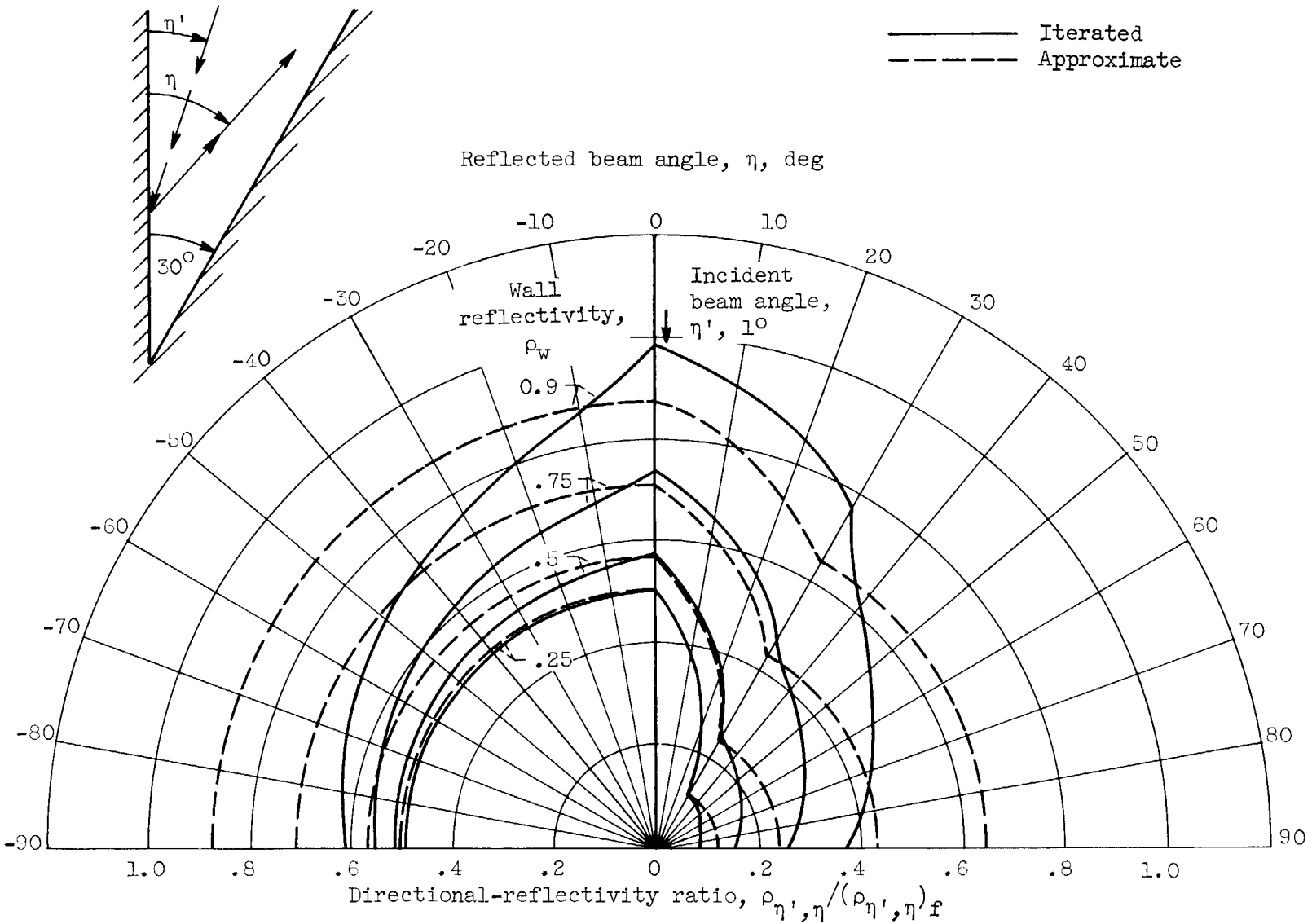

(a) Incident beam angle, 1°.

Figure 8. - Effect of wall reflectivity on directional-reflectivity ratio. Groove angle, 30°.

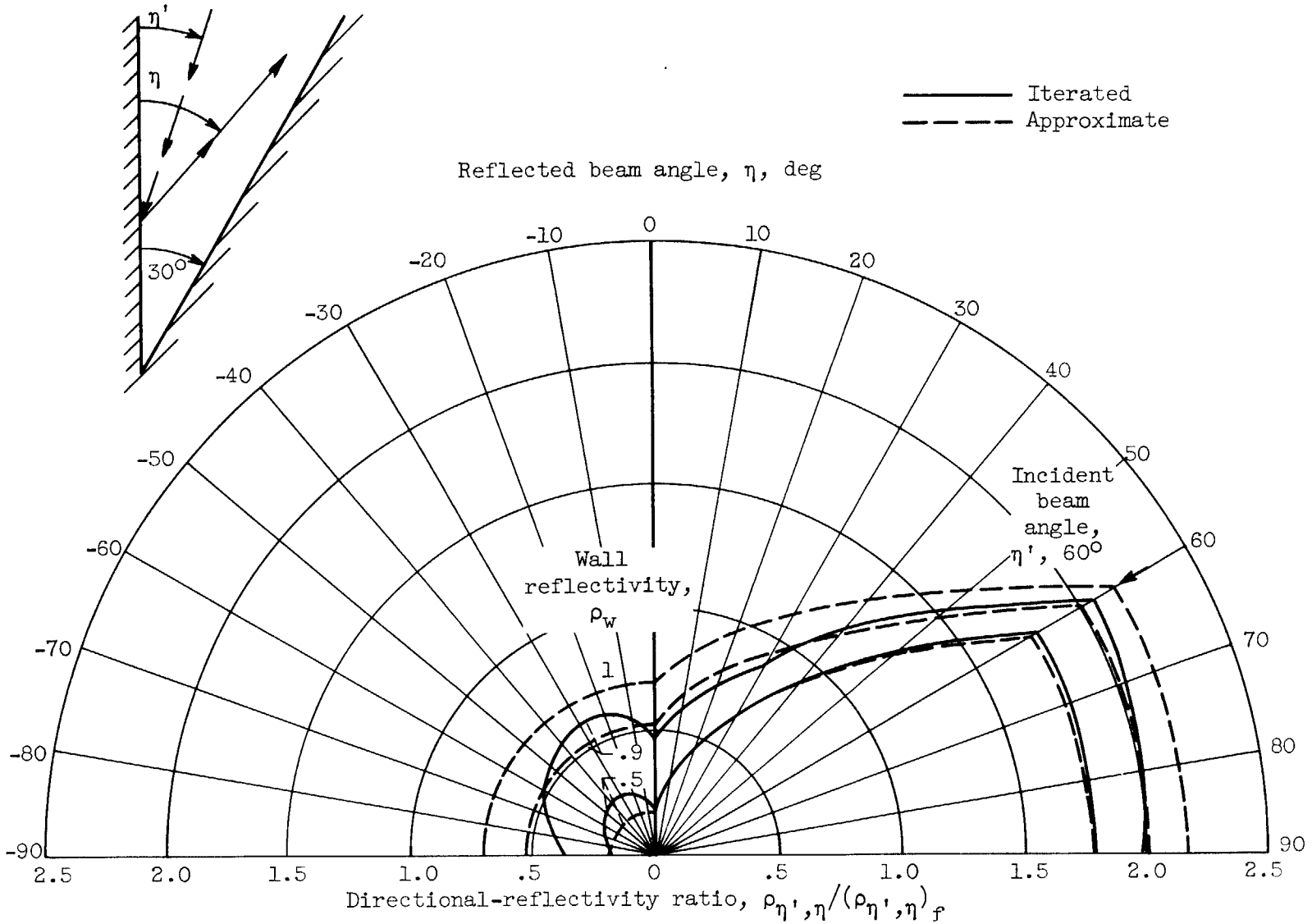

(b) Incident beam angle, 60°.

Figure 8. - Continued. Effect of wall reflectivity on directional-reflectivity ratio. Groove angle, 30°.

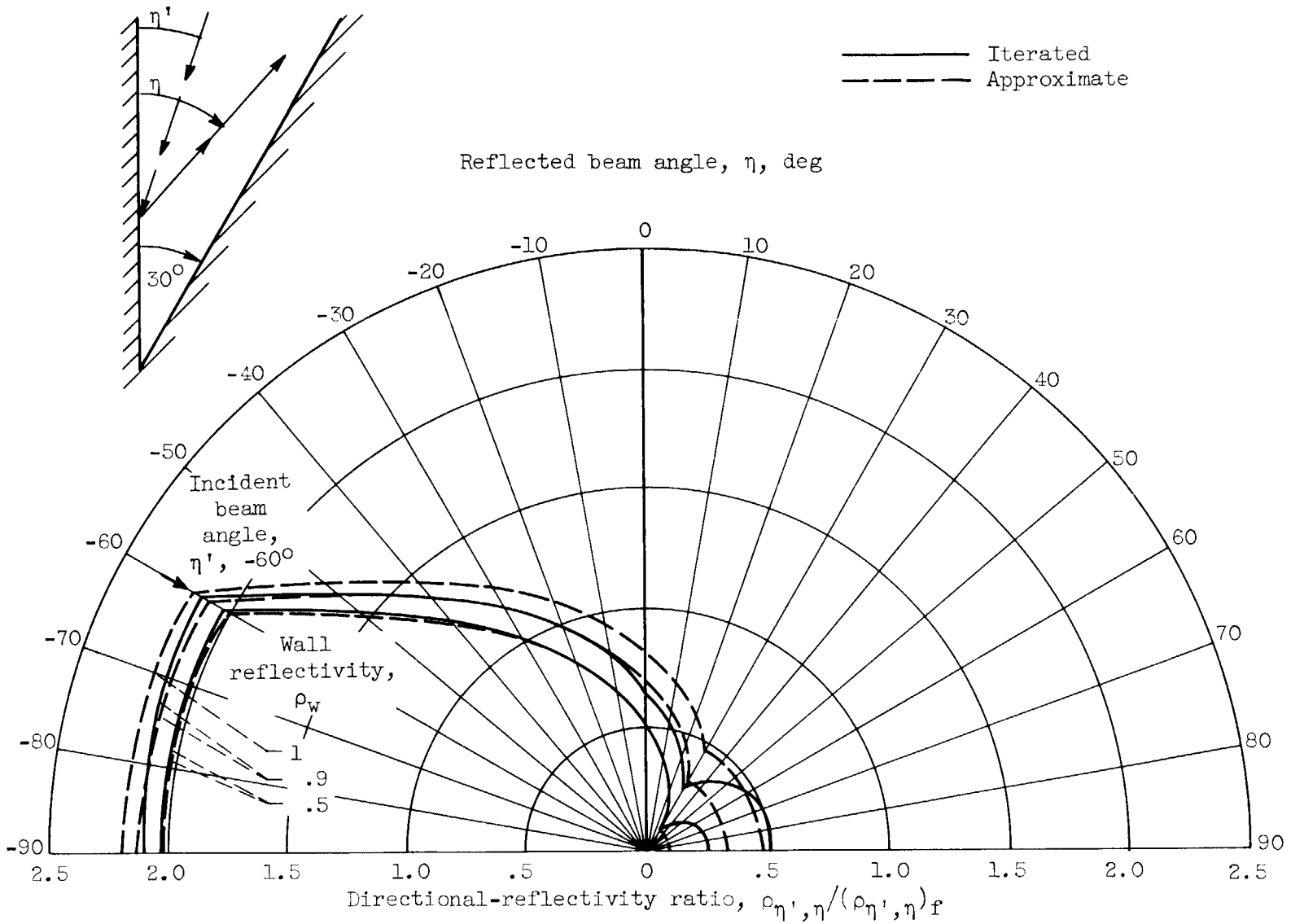

(c) Incident beam angle, -60°.

Figure 8. - Concluded. Effect of wall reflectivity on directional-reflectivity ratio. Groove angle, 30°.

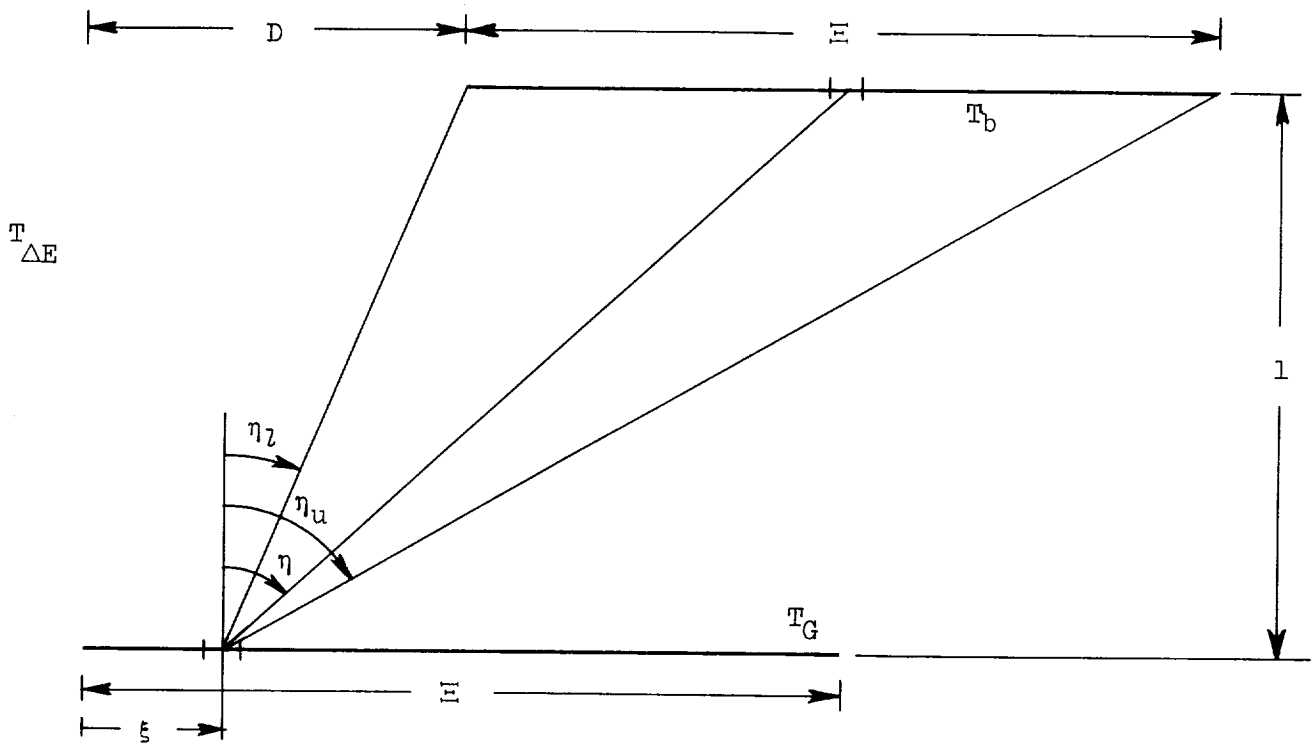

Figure 9. - Radiant heat interchange among a black surface, a directional surface, and the environment.

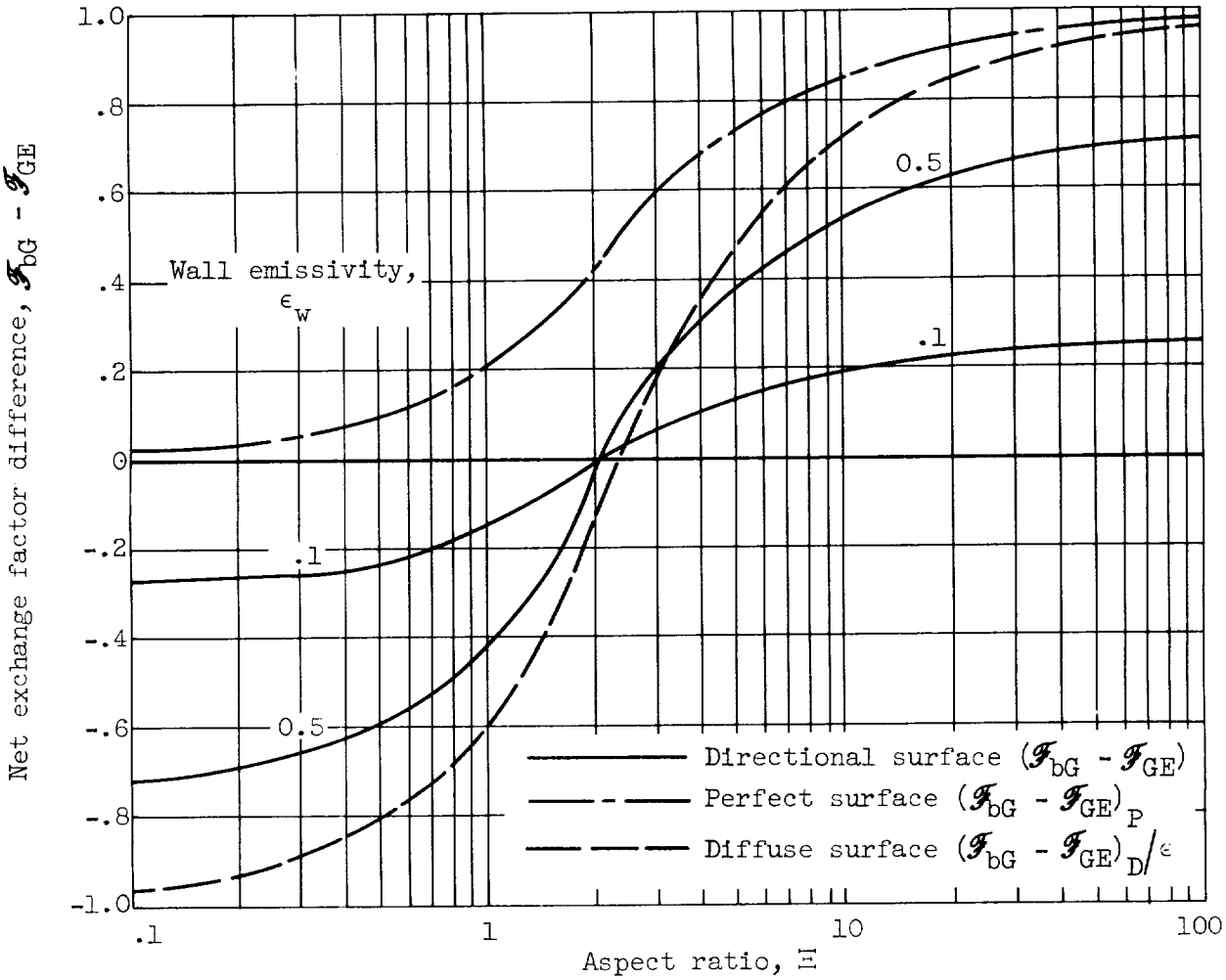

(a) Groove angle, 30°; offset distance, 1.

Figure 10. - Net exchange factor difference.

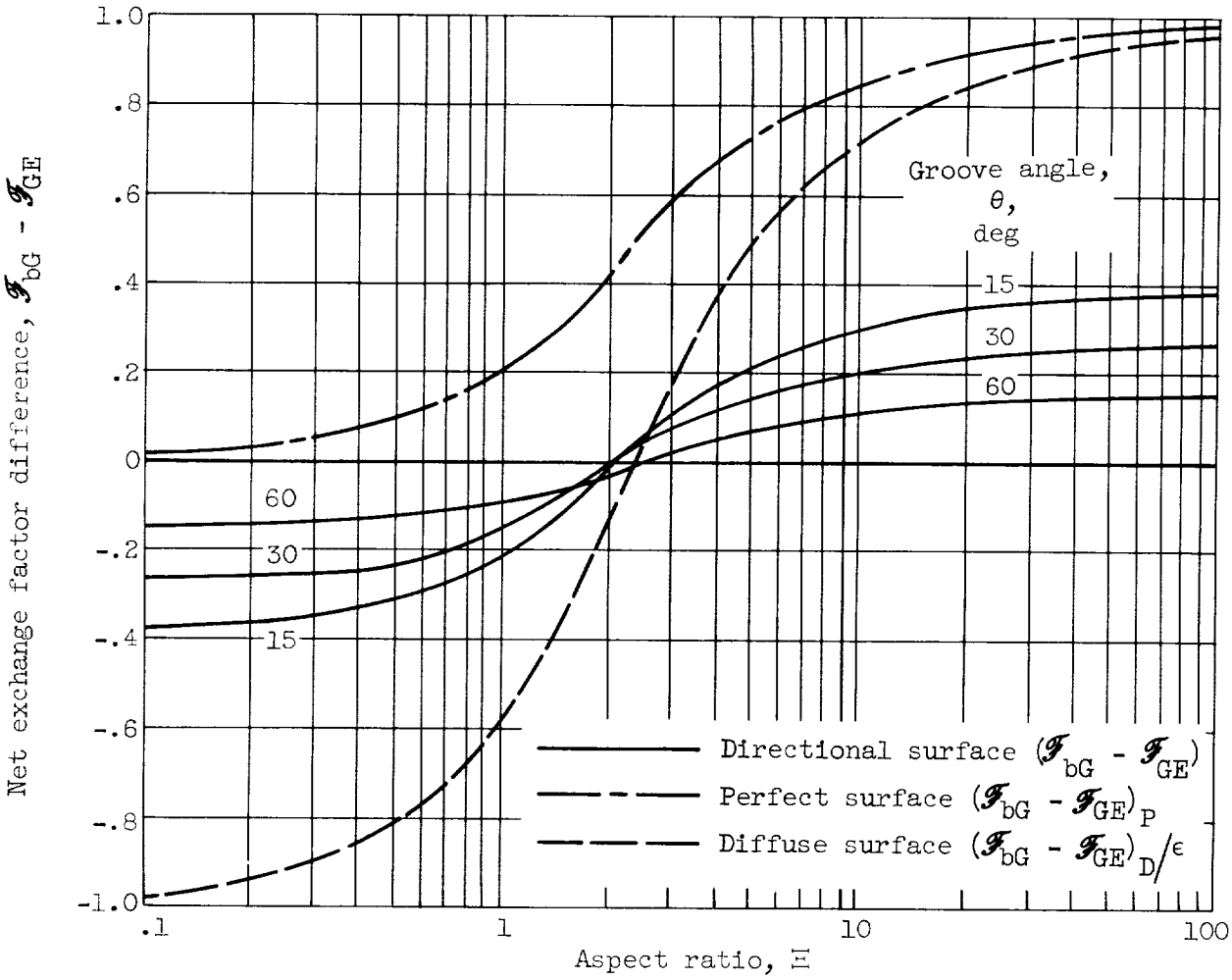

(b) Wall reflectivity, 0.9; offset distance, 1.

Figure 10. - Concluded. Net exchange factor difference.

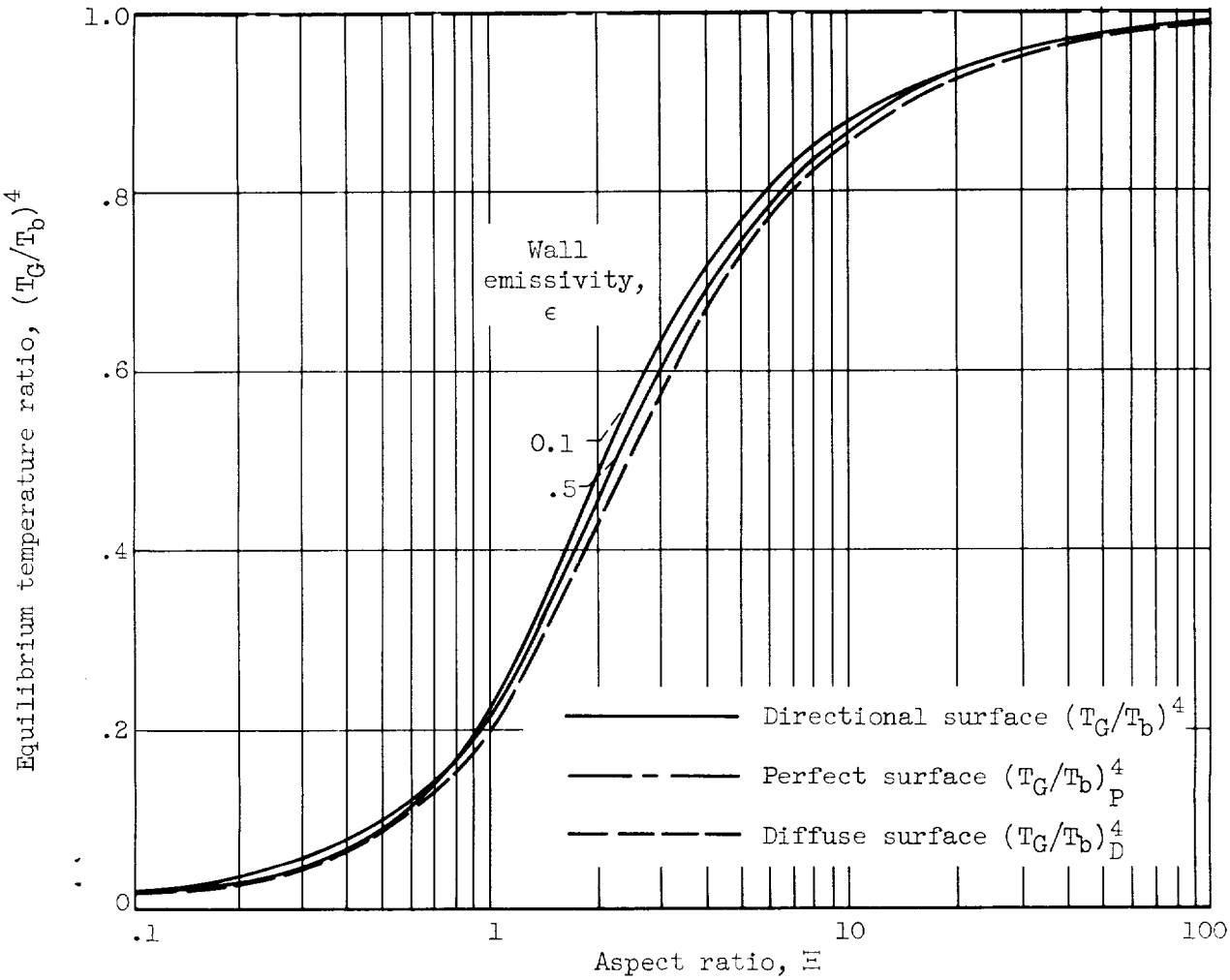

Figure 11. - Equilibrium temperature ratio. Offset distance, l; groove angle, 30°.